DRAFT FINAL REPORT

BDV30 977 — 14

Evaluation of Fog Predictions and Detection, Phase 2

Peter S. Ray. Ph.D.

Florida State University

Department of Earth, Ocean, and Atmospheric Science

Meteorology Program

Tallahassee, Florida 32306

October 2016

DISCLAIMER

"The opinions, findings, and conclusions expressed in this publication are those of the authors and not necessarily those of the State of Florida Department of Transportation."

SI* (MODERN METRIC) Conversion Factors

APPROXIMATE CONVERSIONS TO SI UNITS

SYMBOL	WHEN YOU KNOW	MULTIPLY BY	TO FIND	SYMBOL
LENGTH				
in	inches	25.4	millimeters	mm
ft	feet	0.305	meters	m
yd	yards	0.914	meters	m
mi	miles	1.61	kilometers	km

SYMBOL	WHEN YOU KNOW	MULTIPLY BY	TO FIND	SYMBOL
AREA				
in^2	Square inches	645.2	square millimeters	mm^2
ft^2	Square feet	0.093	square meters	m^2
yd^2	square yard	0.836	square meters	m^2
ac	acres	0.405	hectares	ha
mi^2	square miles	2.59	square kilometers	km^2

SYMBOL	WHEN YOU KNOW	MULTIPLY BY	TO FIND	SYMBOL
		VOLUME		
fl oz	fluid ounces	29.57	milliliters	mL
gal	gallons	3.785	liters	L
ft^3	cubic feet	0.028	cubic meters	m^3
yd^3	cubic yards	0.765	cubic meters	m^3
NOTE: volumes greater than 1000 L shall be shown in m^3				

SYMBOL	WHEN YOU KNOW	MULTIPLY BY	TO FIND	SYMBOL
		MASS		
oz	ounces	28.35	grams	g
lb	pounds	0.454	kilograms	kg
T	short tons (2000 lb)	0.907	megagrams (or "metric ton")	Mg (or "t")

SYMBOL	WHEN YOU KNOW	MULTIPLY BY	TO FIND	SYMBOL
		TEMPERATURE (exact degrees)		
^oF	Fahrenheit	5 (F-32)/9 or (F-32)/1.8	Celsius	^oC

SYMBOL	WHEN YOU KNOW	MULTIPLY BY	TO FIND	SYMBOL
		ILLUMINATION		
fc	foot-candles	10.76	lux	lx
fl	foot-Lamberts	3.426	candela/m^2	cd/m^2

SYMBOL	WHEN YOU KNOW	MULTIPLY BY	TO FIND	SYMBOL
FORCE and PRESSURE or STRESS				
lbf	Pound force	4.45	newtons	N
lbf/in^2	Pound force per square inch	6.89	kilopascals	kPa

APPROXIMATE CONVERSIONS TO SI UNITS

SYMBOL	WHEN YOU KNOW	MULTIPLY BY	TO FIND	SYMBOL
LENGTH				
mm	millimeters	0.039	inches	in
m	meters	3.28	feet	ft
m	meters	1.09	yards	yd

SYMBOL	WHEN YOU KNOW	MULTIPLY BY	TO FIND	SYMBOL
AREA				
mm^2	square millimeters	0.0016	square inches	in^2
m^2	square meters	10.764	square feet	ft^2
m^2	square meters	1.195	square yards	yd^2
ha	hectares	2.47	acres	ac
km^2	square kilometers	0.386	square miles	mi^2

SYMBOL	WHEN YOU KNOW	MULTIPLY BY	TO FIND	SYMBOL
VOLUME				
mL	milliliters	0.034	fluid ounces	fl oz
L	liters	0.264	gallons	gal
m^3	cubic meters	35.314	cubic feet	ft^3
m^3	cubic meters	1.307	cubic yards	yd^3

SYMBOL	WHEN YOU KNOW	MULTIPLY BY	TO FIND	SYMBOL
MASS				
g	grams	0.035	ounces	oz
kg	kilograms	2.202	pounds	lb
Mg (or "t")	megagrams (or "metric ton")	1.103	short tons (2000 lb)	T

SYMBOL	WHEN YOU KNOW	MULTIPLY BY	TO FIND	SYMBOL
TEMPERATURE (exact degrees)				
^{o}C	Celsius	1.8C+32	Fahrenheit	^{o}F

SYMBOL	WHEN YOU KNOW	MULTIPLY BY	TO FIND	SYMBOL
ILLUMINATION				
lx	lux	0.0929	foot-candles	fc
cd/m^2	candela/m^2	0.2919	foot-Lamberts	fl

SYMBOL	WHEN YOU KNOW	MULTIPLY BY	TO FIND	SYMBOL
FORCE and PRESSURE or STRESS				
N	newtons	0.225	poundforce	lbf
kPa	kilopascals	0.145	poundforce per square inch	lbf/in^2

*SI is the symbol for the International System of Units. Appropriate rounding should be made to comply with Section 4 of ASTM E380.
(Revised March 2003)

Technical Report Documentation Page

1. Report No. BDV30 977 — 14		3. Recipient's Catalog No.

4. Title and Subtitle **Evaluation of Fog Predictions and Detection Phase 2**	5. Report Date 9/01/2016 6. Performing Organization Code
7. Author(s) **Peter S. Ray, PhD**	8. Performing Organization Report No.
9. Performing Organization Name and Address **Department of Earth, Ocean and Atmospheric Sciences** **Florida State University**	10. Work Unit No. (TRAIS) 11. Contract or Grant No. BDV30 977 — 14
12. Sponsoring Agency Name and Address **Florida Department of Transportation**	13. Type of Report and Period Covered **Final Report** 14. Sponsoring Agency Code

15. Supplementary Notes

16. Abstract

On January 29, 2012 at about 4:00 am a thick fog and smoke caused a multiple car crash just south of Gainesville, Florida. 11 people were killed and 18 were hospitalized. Nationally there are about 38,000 fog related accidents which result in about 620 fatalities. It would be valuable to anticipate where and when fog will form. It that is through numerical models, the environmental factors are the requisite input. One of these is soil moisture. It is found a very economical way with no loss is accuracy is to use NWS collected radar accumulated rainfall instead of expensive soil measurements.

17. Key Word **Radar Rainfall, Measurement of Soil Moisture, Fog Formation, Remote Sensing,**	18. Distribution Statement

19. Security Classif. (of this report) **Unclassified**	20. Security Classif. (of this page) **Unclassified**	21. No. of Pages	22. Price

Executive Summary

Fog or fog enhanced with smoke has been shown to reduce visibility to levels where diving is unsafe. Numerous pre-dawn accidents attest to this fact. The solution is to be able to slow or redirect traffic to avoid unsafe speeds in low visibility conditions. Even more desirable would to be able to anticipate those emerging conditions.

The desire is to be able to forecast fog formation and also to detect fog formation. This effort is to provide data on one component that is thought to be important in the ability to forecast fog formation. One such variable is that of soil moisture. It is impractical to have instrumentation at all the possible fog locations. Not only would it be expensive to install, but the maintenance cost makes it nearly prohibitive. Thus, some constantly vigilant mechanism would be desirable. Remote sensing offers such a capability.

We examined the use of NWS network Radar rainfall data, available at no cost, to assess whether it can be used to derive soil moisture. This is an innovative approach, not previously discussed in the literature. Since Florida only has 6 stations that measure and archive soil moisture, we used data from Oklahoma and their 86 operational mesonet stations to verify the algorithm. It was found that radar derived accumulated rainfall was an accurate predictor of soil moisture. This was then used to illustrate what is possible and could be routinely implemented in Florida or any other state. This then provides tens of thousands of data points of soil moisture in any state, including Florida in a fog prediction algorithm.

TABLE OF CONTENTS

LIST OF FIGURES

ACRONYMS

AMS	American Meteorological Society
ASOS	Automated Surface Observing System
AVHRR	Advanced Very High Resolution Radiometer
AWOS	Automated Weather Observing System
CCN	Cloud Condensation Nuclei
FDOT	Florida Department of Transportation
FSU	Florida State University
GOES	Geostationary Operational Environmental Satellite
GVAR	GOES Variable
IR	Infrared
MADIS	Meteorological Assimilation Data Ingest System
McIdas	Man computer Interactive Data Access System
NASA	National Aeronautics and Space Administration
NDVI	Normalize Difference Vegetation Index
NESDIS	National Environmental Satellite, Data, and Information Service
NOAA	National Oceanic and Atmospheric Administration
NWS	National Weather Service
RH	Relative Humidity
SW	Short Wave
TLH	Tallahassee, Florida
UTC	Coordinated Universal Time

1. INTRODUCTION

1.1 The Problem

On November 22, 2012, at about 8:35 a.m., a thick fog resulted in a 140-car accident near Beaumont, Texas. Remarkably, only two people died and eighty people were injured and required hospital care. On January 29, 2012, about 4:00 a.m., amidst thick fog and smoke on I-75 south of Gainesville, Florida, 11 people were killed and 18 hospitalized in a multi-car crash. Nationally, there are about 38,000 fog related car accidents ea year resulting in about 620 fatalities. In Florida, between 2002 and 2009, 299 people died in vehicle crashes related to fog and smoke conditions on Florida highways. This is more than the amount of deaths in Florida caused by hurricanes and lightning combined.

1.2 The Nature of Fog

Fog is a cloud located near ground level. All types of fog require ubiquitous cloud condensation nuclei (CCN) and can form with a relative humidity less than 100%. The opaqueness (heaviness or thickness) of fog may be substantially increased by the presence of smoke, due to the increase of CCN. Fog is both spatially and temporally variable.

With observation equipment widely dispersed, the challenge is how to forecast the occurrence of fog from observation far removed from the location of fog occurrence. With the available observation data from 2002 to 2009, the location and frequency of fog was determined, thus forming a fog climatology by Ray et al. (2014) and with the use of geosynchronous satellite data, a new higher resolution climatology was determined by Ray and LeFran (2015) . Ray et. al. (2014) also detailed the conditions under which fog would form. Based on data from those study, researchers evaluated fog prediction techniques and made recommendations for improving fog-warning systems along Florida's highways.

The definition of fog is an observed visibility below one kilometer resulting from the presence of suspended water droplets and/or ice crystals (National Oceanic and Atmospheric Administration or NOAA, 1995). According to Houghton (1985), fog generally occurs when water droplets are suspended in air that is within ten percent of saturation. Typically, there are three primary physical processes that can make unsaturated air become saturated. These include cooling the air temperature, adding moisture, and mixing air parcels with different humilities and temperatures vertically (Duynkerke, 1990). There are many other atmospheric and localized factors that can exacerbate these mechanisms; including vegetation, horizontal and vertical winds, radiation fluxes, soil moisture, and topographic effects. However, once fog has formed, the primary mechanisms influencing further fog development and intensity are radiational cooling, gravitational droplet settling, fog microphysics, and cloud cover (Duynkerke, 1990).

1.3 Types of fog

Synoptic, dynamic, and microphysical conditions will normally control what type of fog will generally form. Willett (1928) created an all-inclusive fog classification system, later revised by Byers (1959), which comprised 11 different types of fog, each of which was categorized by the physical processes involved and the atmospheric scenario in which the fog formed. Most of the fog types classified by Byers (1959), however, are merely derivatives of the four distinct types of fog as described by Stull (1999): advection fog, upslope fog, frontal fog, and radiation fog. This project will focus primarily on the two types of fog found in the state of Florida, radiation fog and advection fog.

1.3.1 Advection Fog

Advection fog occurs when a warm moist air mass moves over a cool surface (AMS, 1999). The warmer air mass loses heat through conduction to the cooler surface, thus lowering its temperature to its dew point temperature (Stull, 1999). The surfaces on which advection fog can form include: cold water, cold ground, and ground covered with snow or ice. Advection fog is typically found in marine environments such as coastal areas, as water sources provide the moisture and heat necessary to facilitate this fog type. In Florida, advection fog is formed sometime along the coastline, most frequently the Gulf coast. It rarely penetrates more than a mile inland.

1.3.2 Radiation Fog

Radiation fog forms when radiative fluxes off the surface are sufficient to reduce the air temperature to its dew point (AMS, 1999). This fog type forms at night and typically requires clear skies and abundant low-level moisture. Clear skies are necessary in order for long-wave radiation to escape from the earth's surface, allowing temperatures to decrease rapidly. If dew point temperatures are sufficiently high enough, humidity levels can reach a critical point where fog will form. In addition, light winds, typically below 2.5 m/s (Taylor, 1917), are also necessary for radiation fog to occur. If wind speeds are too strong, turbulence within the boundary layer will result, and low-level moist air would mix with drier air aloft. However, if winds are too calm, gravity will force the suspended water droplets to settle on the ground, creating dew/frost. Other favorable conditions for radiative fog formation include a small dew point depression at sunset, low-lying areas or valleys, and large amounts of condensation nuclei.

Radiation fog forms upward from the ground as the night progresses and is usually deepest and most opaque around sunrise. Initially, the fog density decreases with height as temperatures at low-levels increase with height. However, as the fog continues to thicken at lower levels, it restricts the surface/ground from emitting long-wave radiation. When conditions reach this point, the maximum radiative cooling level moves upward toward the top of the fog layer. This results in denser fog at the top of the layer and initiates sinking cold thermals that act to turbulently mix the fog (Stull, 1999). Radiative cooling at the top of the fog can act to maintain and strengthen the fog intensity (Stull,1999).

Radiation fog generally begins dissipating when the sun rises in the early morning hours, initiating mixing in the boundary layer. Through this method the surface warms quickly as it absorbs short-wave radiation and then warms the surrounding air. The water vapor droplets easily evaporate into the warmer air, resulting in dissipation of the fog. Radiation fog can also dissipate if there is a change in the overlying synoptic conditions, such as fronts or winds, or the dynamic forcing is altered. In the southern United States, this type of fog is most problematic during the winter because the length of night is sufficiently long enough to drop the air temperature to the dew point. Interestingly, and as yet inexplicably, Tallahassee, Florida seems to be an exception to this, as it experiences more fog days during summer months.

The above classification of fog highlights some of the scenarios under which fog forms. However, it doesn't provide a clear depiction of the dynamics and physical processes involved due to its high time and spatial variability. Thus, the complex nature of fog is difficult to detect and forecast. Regardless, fog is still a boundary layer phenomenon so its formation and influences can be better understood through climatic studies of surface conditions. Approximately 90% of all fog and the fog most associated with traffic accidents in Florida are of this type.

For radiation fog to form, the primary conditions are:

1. The winds must be near zero or very light. One rule of thumb is less than 4 m/s. This is because if the winds were stronger it would encourage mixing and the temperature rising (and the relative humidity falling) because of the mixing to near the ground of warmer air from aloft.
2. Relative humidity increases by either cooling the air and thus raising the RH

because cool or cold air can not hold as much moisture as warm air, or by adding moisture to the air by evaporation.

1.4 Previous Climatologies

1.4.1 Surface Stations. Up until recently all the fog climatologies relied either heavily or exclusively on the NWS reporting stations, which are places 100s of miles apart.

Some of the earliest climatologies

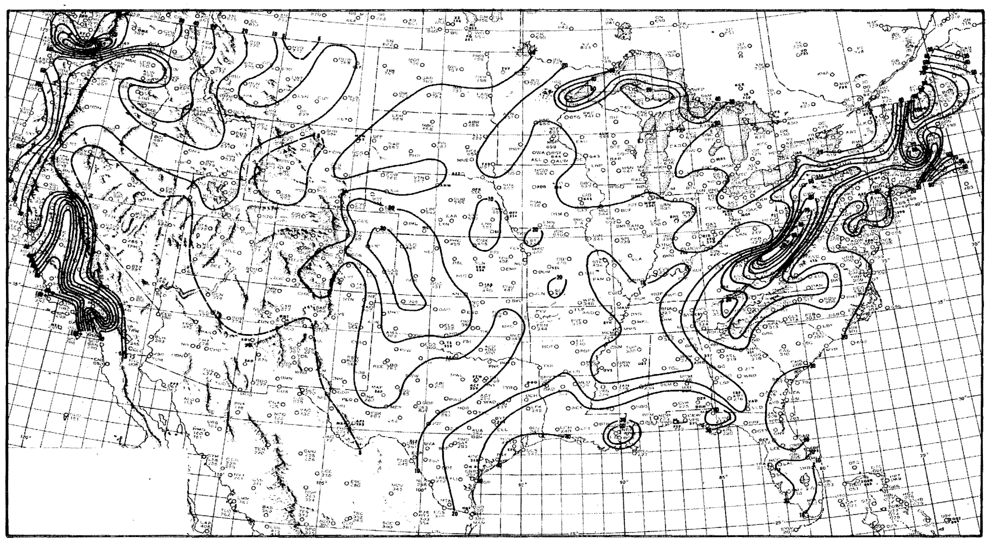

Fig. 1.1 Fog frequency in the United States (from Stone, 1936)

Another climatology was published in 1969 by Peace and is shown in Fig. 1.2.

This was followed by another climatology in 1973. All of these have similar rates but constrained by weak data. The weather station in the in the central Florida panhandle was located north of Apalachicola. It was not moved to Tallahassee until the early 1990s.

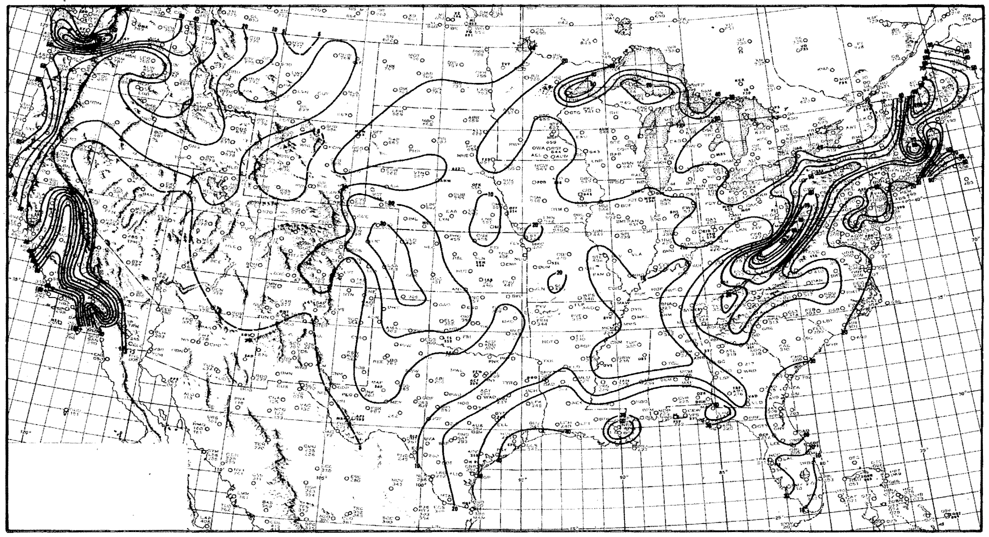

Fig. 1.2 Fog frequency in the United States (from Peace, 1969)

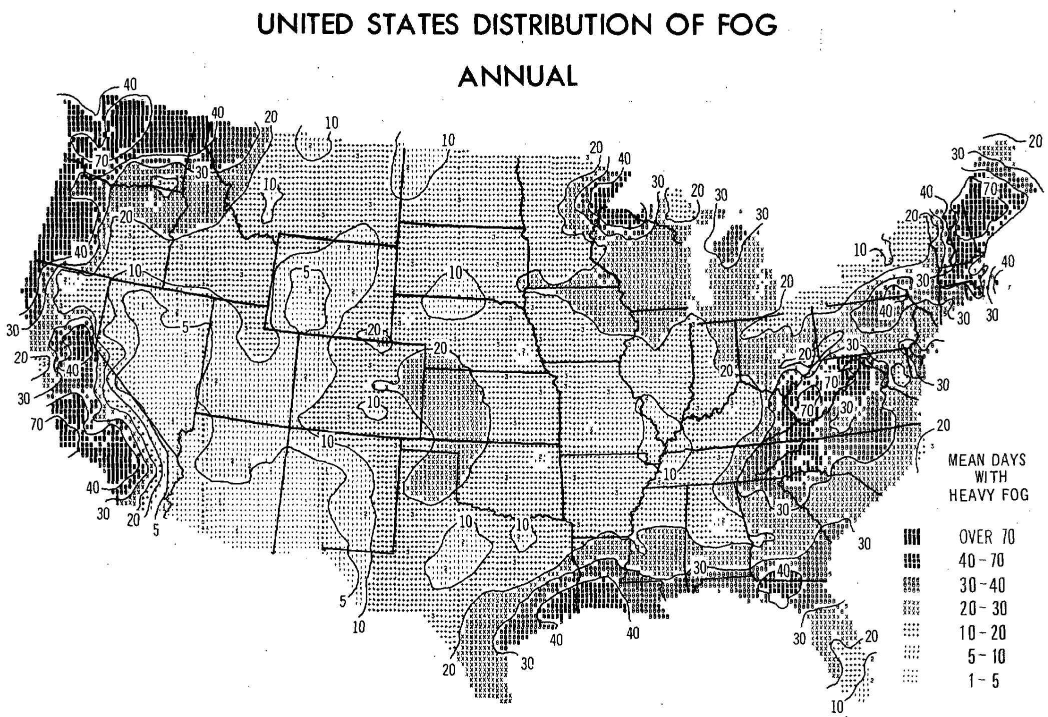

Fig. 1.3 Annual fog frequency in the USA (from Hardwick, 1973)

Croft et al. (1997) focused on the Southern US, specifically Alabama, Louisiana and Mississippi, and uses local and regional climatic studies of fog combined with numerical models, soundings, satellite imagery and diagnostic software to forecast fog. The study found that in this region, the greatest average number of dense fog days occurs near the coastline and in the cool season, with the highest percentage of fog occurrence during the early morning hours.

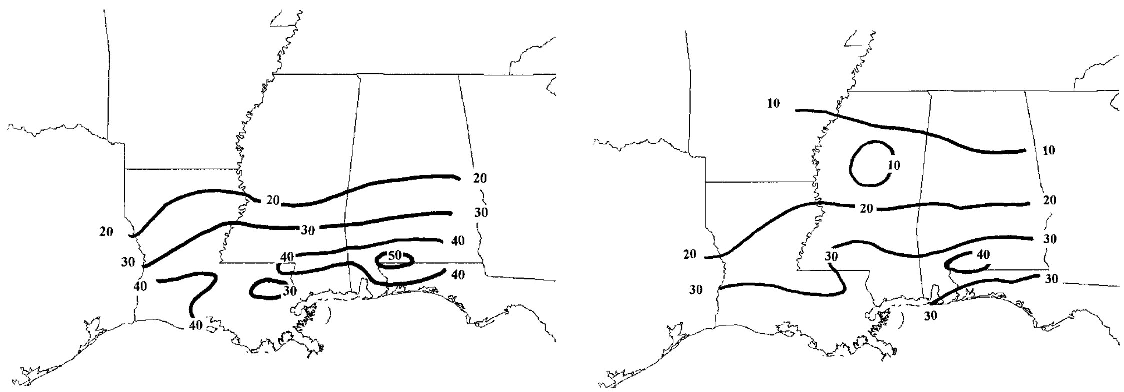

a b

Fig. 1.4 Fog climatology from Croft, (1997) for the cold season (a) and the warm season (b)

Forthun et al. (2006) obtained Hourly Surface Airways datasets from 1948-2003 for 26 stations in the Southeastern US and performed a linear regression on the dataset to examine annual and seasonal trends in the number of fog event days and fog duration. A variation of trends was reported in the southeast US, however decreasing trends were dominant. Six of these stations were located in Florida: Tallahassee, Jacksonville, Daytona Beach, Tampa, Palm Beach and Miami. The study found that four of the six Florida stations (DAB, JAX, MIA, TPA) showed significant decreasing/increasing trends in fog event days over the time period. Seasonally, TLH displayed no significant trends in any season. While they could not correlate the effect of land use, geography and population density to the trends in fog events, the study did show that the majority of fog days occurred in the winter, followed by autumn, spring and summer. These results line up with those done by Hardwick (1973) and Court and Gerston (1966), which indicate January as the peak fog month for most of the Southeast US.

Ray et al. (2014) conducted a study that comprehensively looks at the climatology of fog in Florida. A five-year climatology of fog in Florida was undertaken. It used the only data available, the 75 ASOS and AWOS stations that have visibility sensors. The locations of these are shown in Fig. 1.

The results from Ray et al. (2014) study are presented in Figs. 1.5 This figure shows that, while fog is highly variable spatially, it often tends to form in preferred locations. The ASOS/AWOS ground stations are not always sited to detect local fog locally, and certainly not its areal extent, however observations from these sites were used to develop a fog climatology for Florida. The period coved encompasses 65 years.

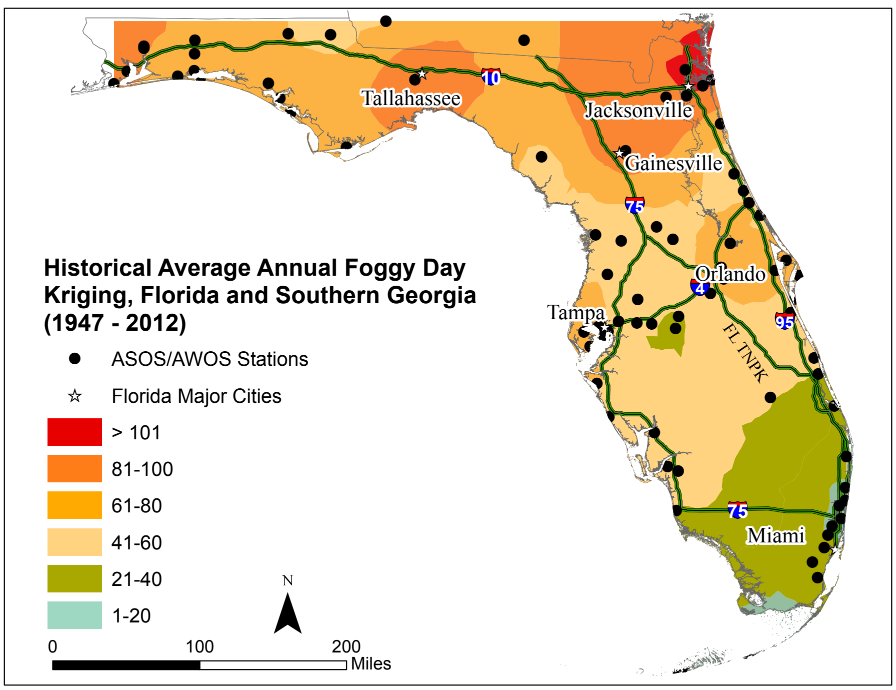

Fig. 1.5. Fog or foggy days in Florida based on a sixty five year climatology. Location of surface station are given by black dots. (Ray and Rivard, 2014).

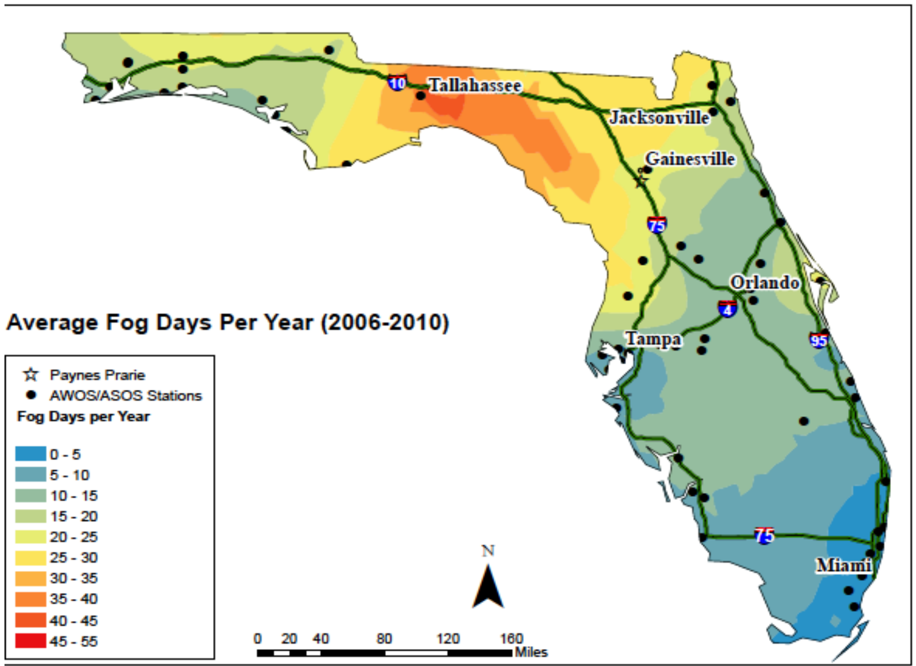

Fig. 1.6 A five year fog climatology for the years 2006-2010. (from Ray and Rivard (2014).

As shown in Ray et al. (2014), and reproduced here in Fig. 1.7, the fog climatology was constructed for the year 2012, the year that is the focus of this research.

1.4.2 Satellite detection of fog

Ground-based observations provide accurate assessments of visibility and cloud cover for a specific location. But this form of data is discontinuous and can be sparse. Even if ground-based or station data was available at a high spatial density, interpolating the data can be moot due to fog formation being a complex phenomenon influenced by multiple factors (Cermak et al, 2009). Overall, satellite data provides supplementary information on the horizontal coverage of fog.

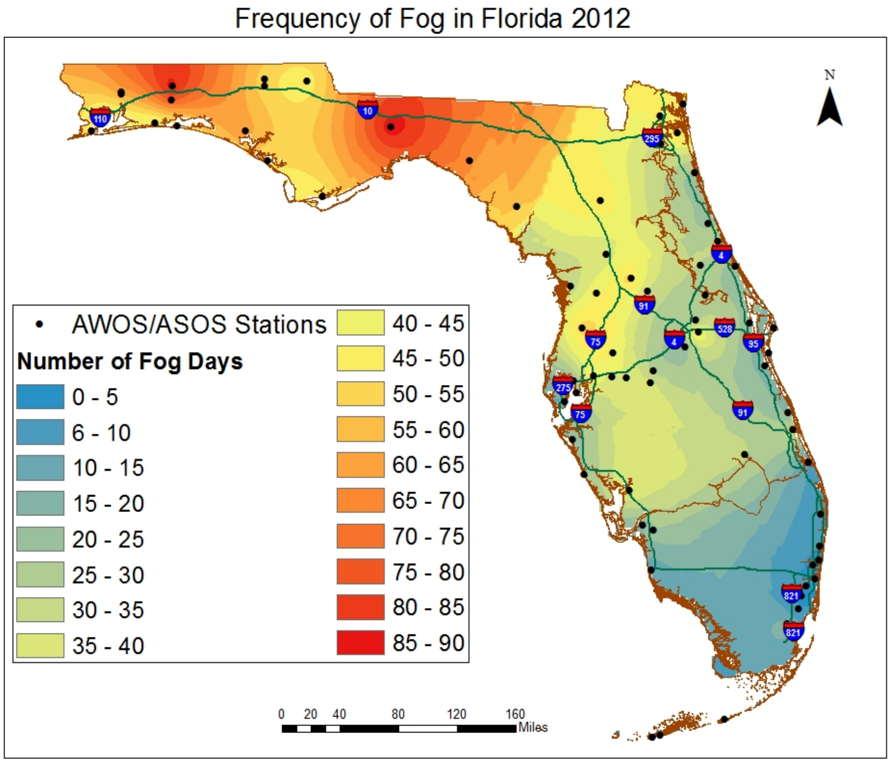

Fig. 1.7 Fog days for that year 2012 from the ASOS/AWOS stations. This can be compared to the more extensive data sets give in Figs. 1.2 and 1.3

Hunt (1973) theoretically determined two factors that lead to differences in the radiative properties of clouds in various visible and IR wavelengths of the spectrum. The first factor is due to fog droplets being less emissive in the 3.9-µm wavelength than in the 10.7-µm wavelength, whereas both emissivities are approximately the same for larger cloud droplets. This difference in emissivity between the long-wave and short-wave IR channel is what causes a difference in temperature readings of a cloud observed by a satellite. The second factor is due to emissivity differences allowing for more radiation from below the cloud top to be sensed in the longwave IR channel. This is why at night liquid low-level clouds appear colder in the SW IR channel than in the LW IR channel due to low transmissivity in the SW IR part of the spectrum. Meanwhile, thin ice-phase cirrus clouds appear warmer in the SW IR channel due to higher transmissivity. Cloud free areas will usually have a small temperature difference between the SW and LW IR channels due to differential water vapor absorption (Findlater 1985). The above radiative properties of cloud were applied to remote sensing techniques. These findings paved the way for satellite fog detection techniques where the difference in brightness temperatures between two wavelengths for a pixel is tested against a threshold value and classified as either low stratus (fog)/clear/other cloud.

The first attempt at nighttime fog-detection using multispectral IR images was in Great Britain by Eyre et al (1984). Advanced Very High Resolution Radiometer (AVHRR) imagery onboard a NOAA polar-orbiting satellite was used. It produced imagery in three IR bands, one visible band and one near-IR spectral band at a 1.1 km spatial resolution. Temperature differences between channel 3 centered near 3.7-μm and channel 4 centered near 11.0-μm were used for fog detection. Temperature differences greater than 2.5 K signaled opaque clouds layer, temperature differences less than 0.5 K signaled an absence of clouds, and temperature differences between these two thresholds signaled either semitransparent fog or cloud. This methodology was soon after applied in the United States using AVHRR imagery (d'Entremont, 1986).

The nighttime dual channel fog detection technique was used on a wide arrange of platforms, including geostationary instruments. Lower resolution imagery from GOES-7 also proved to be capable of a nighttime bi-spectral fog detection technique (Ellrod et al., 1989). It had an onboard radiometer called the Visible and Infrared Spin Scan Radiometer (VISSR) Atmospheric Sounder (VAS), with the equivalent to the AVHRR channel 3 and 4 being channel 12 (3.9-μm) and channel 8 (11.2-μm), respectively. CH-8 was produced every 30 minutes and CH-12 was produced hourly. Even though CH-8 had a sub point resolution of 6.9 km and CH-12 had a sub point resolution of 13.8 km, both could still be used to derive an image detecting larger regions of fog or low clouds at night (Montgomery and Uccellini, 1985).

In April of 1994, GOES-8 was launched. It was the first satellite in the advanced GOES I-M series, which would provide imagery in the 3.9-µm and 10.7-µm IR windows (channels 2 and 4 respectively) at a sub-point resolution of 4.0 km (Menzel and Purdom, 1994). Not only was there a significant improvement in resolution in GOES-8, there was also an improvement in frequency of data scans. Separation of the imager and sounder instruments in GOES-8 allowed for imagery in both channels to be available at 15-30 min intervals. Instrument noise was also reduced. Ellrod (1995), used the bispectral IR image differencing technique on both GOES-7 and GOES-8 IR imagery and found it efficient in detecting fog/stratus over a wide variety of land and temperature regimes, as long as the fog wasn't obscured by overlying clouds (Underwood et al., 2004). Lower resolution GOES-7 imagery did demonstrate limitations in the detection of small and narrow areas of fog.

During daylight, sunlight reflected by liquid water clouds adds to the total observed radiance in the 3.9-µm wavelength. The SW IR window's sensitivity to radiation causes the 3.9-µm temperatures to be larger (warmer) than the 10.7-µm temperatures, so the liquid water clouds signal a negative temperature difference. Consequently, fog product becomes less useful during daytime hours. Fog and low clouds can be observed in the visible imagery at a high-resolution of 1 km. However, the use of the visible spectrum to detect fog during the daytime has its disadvantages. These include diurnal changes in illumination due to changes in solar elevation and difficulty in the distinction of fog from other highly reflective surfaces such as other types of clouds or snow.

The National Oceanic and Atmospheric Administration (NOAA) manage the country's environmental satellite program. Within NOAA, the National Environmental Satellite, Data, and Information Service (NESDIS) office is responsible for the operation, processing, distribution and archiving of satellite data. The National Aeronautics and Space Administration (NASA) designs, develops and launches the satellite spacecraft. GOES along with POES (Polar orbiting Operational Environmental Satellites) operations, provide a global satellite network. A year's worth of data before local dawn will be used in order to form a climatology of fog in Florida. GOES-13 Infrared (IR) imagery from Geostationary Operational Environmental Satellite (GOES) is used due to its ability to produce images at a high frequency (every 30 minutes or less) and high spatial resolution of approximately 4 km for IR images and 1 km for visible images (Ray and Lefran, 2015). There study utilized data from both GOES 13 and GOES 14. GOES data is available in real-time, but past data is archived and distributed by the NOAA National Climatic Data Center (NCDC). Data is available in a selection of file formats that can be requested and transferred to your operating system. 'Area' files are in a format specific to GOES images, which store the data in GVAR format along with its calibration and navigational information. NOAA has a Weather Toolkit available online which can be downloaded to one's desktop and used for the conversion from Area format to either binary, ASCII, netCDF, or geoTIFF data.

The analysis from Ray and LeFran (2015) provide a one year climatology of fog from the GOES satellite. Many of the same feature as observed independently can be identified. But some of either greater or lesser amounts of fog are not found in other climatologies.

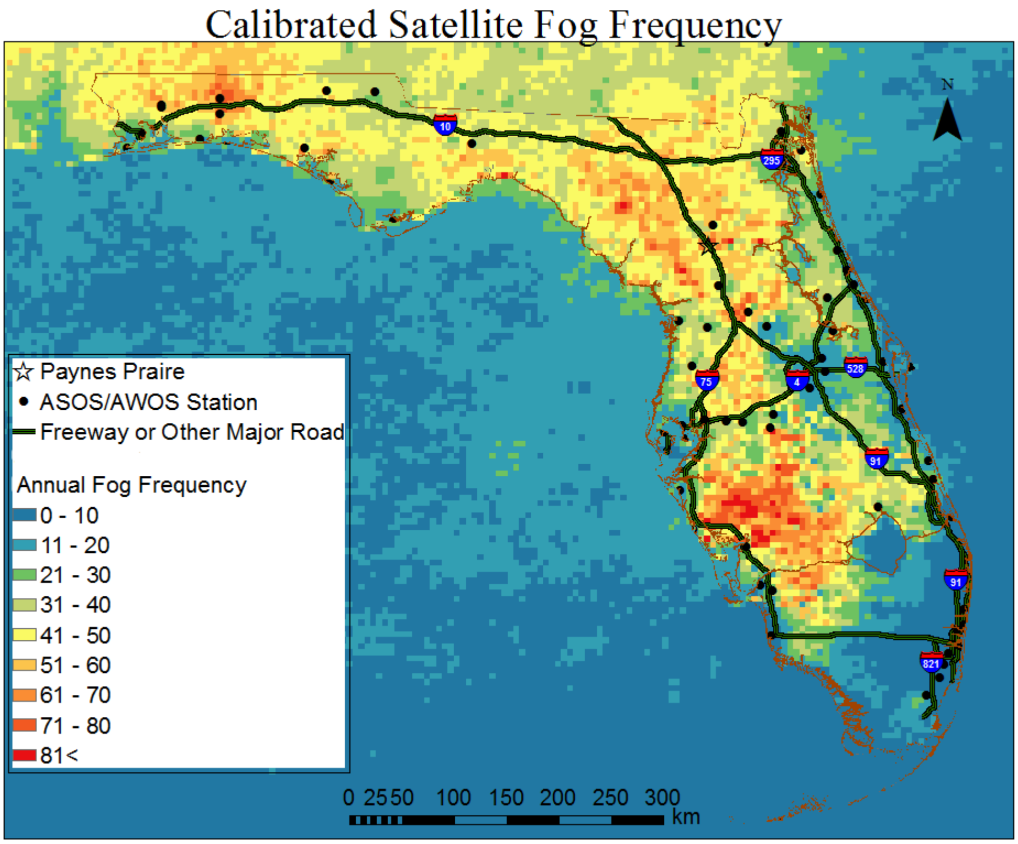

Fig. 1.8 Adjusted GOES satellite image of fog frequency for 2012. The histogram reflects the pixel distribution over Florida.

1.4.3 Inferred presence

In the absence of direct measurement, proxies are often used. The Department of Forestry developed the LOVORI index which is used by the National Weather Service (NWS). The produce high resolution data sets, but only use statewide estimates. The Lovori index is sensitive to the relative humidity and the winds. The results are shown in

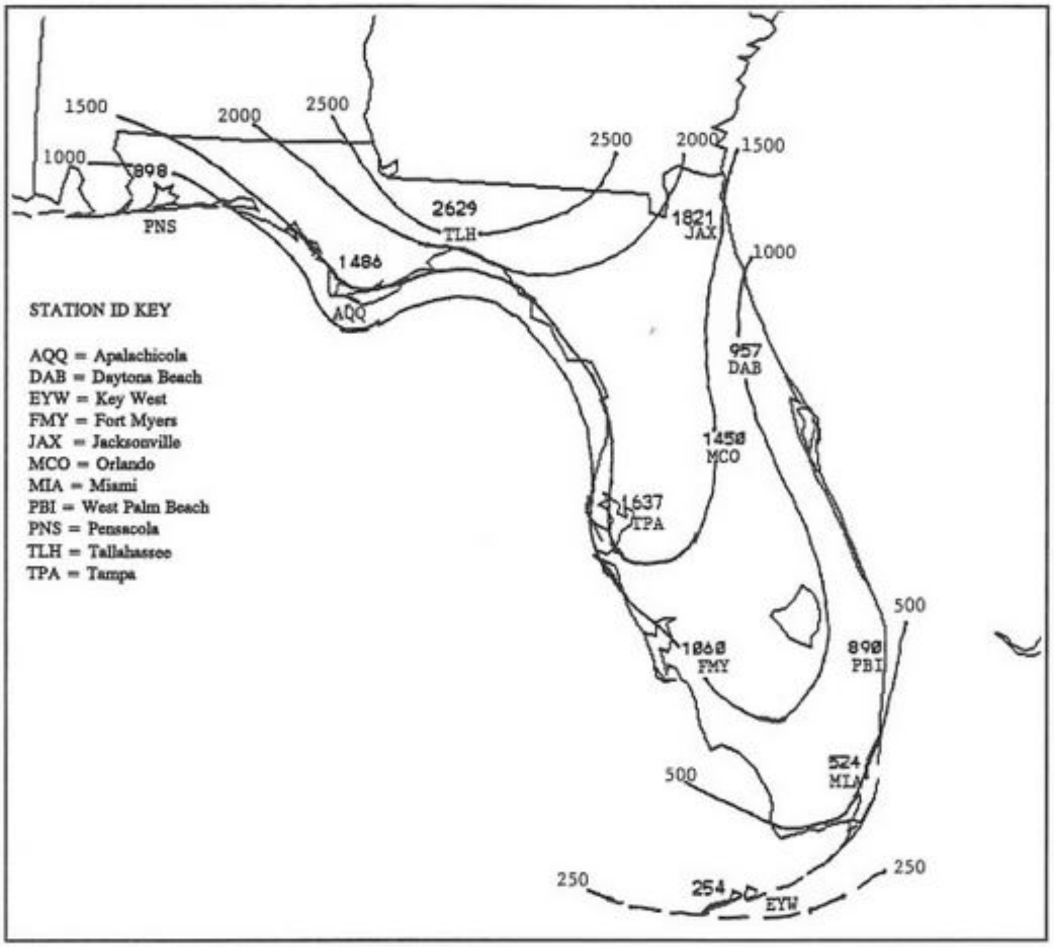

Fig. 1.9 Number of observations (out of 8,768) with LVORI greater than or equal to 7. (From Lavori and Achtemier, 1995)

2. METHODOLOGY

Central to the methodology is to relate and calibrate the radar and satellite data to the observed soil moisture. Since we are concerned on the effect of soil moisture on the emissivity of the ground and the potential of increasing water vapor in the air, only the soil moisture very near the surface is germane. In general, the amount of rain required to saturate the soil and the degree of saturation possible depends on the soil type near the surface and the soil types in the soil column. It also depends on the rainfall that as preceded it, up to the previous 10 days. The soil becomes saturated the same day at 2 inches depth with a few inches of rain. In the absence of rain, it will dry to its dry state within eight to ten days, drying almost ten to twelve percent a day.

The soil moisture is given in the non-dimensional ratio of cubic centimeters of water in a cubic cm of soil. We found that that as long as there was at least half and inch of rain in the past two days, the soil (rather independent from soil type) became saturated. However, the maximum and minimum amount of moisture the soil could hold expressed as a ratio of volume was about .5 at a maximum to .01 as a minimum.

It is the goal of this project to see to what extent that radar data could serve as a proxy for soil moisture measurements. The source of water in the ground comes from the rain. If rainfall can be successfully correlated to the moisture there are several inherent advantages.

1. The resolution would be increased from hundreds square miles to a few kilometers.
2. The cost of collection is borne by the NWS and the data if free compared to hundreds of dollars per sensor after installation.
3. The cost of power and data transmission is eliminated

No doubt the greatest advantage is the increase in resolution and the reduction in cost, if it can be effectively accomplished.

3. DATA SOURCES

The soil type is important and this will be addressed later. Fig. 3.1 shows one (of many) presentations of soil type in the United States. As can be seen in Fig. 3.2 there are only 6 stations in Florida that measure and record soil moisture. Fortunately, Oklahoma has nearly 100 mesonet sites that measure, among other things, soil moisture and rainfall. The mesonet sites in Oklahoma was chosen to develop an robust algorithm to detect the variations in soil moisture and if they could be forecast or determined by the use of NWS network radar data. The location of these stations is illustrated in Fig. 2.1 and given in Appendix A They also are identified by one of 9 soil types. Once a robust algorithm was established, then it could be applied to Florida.

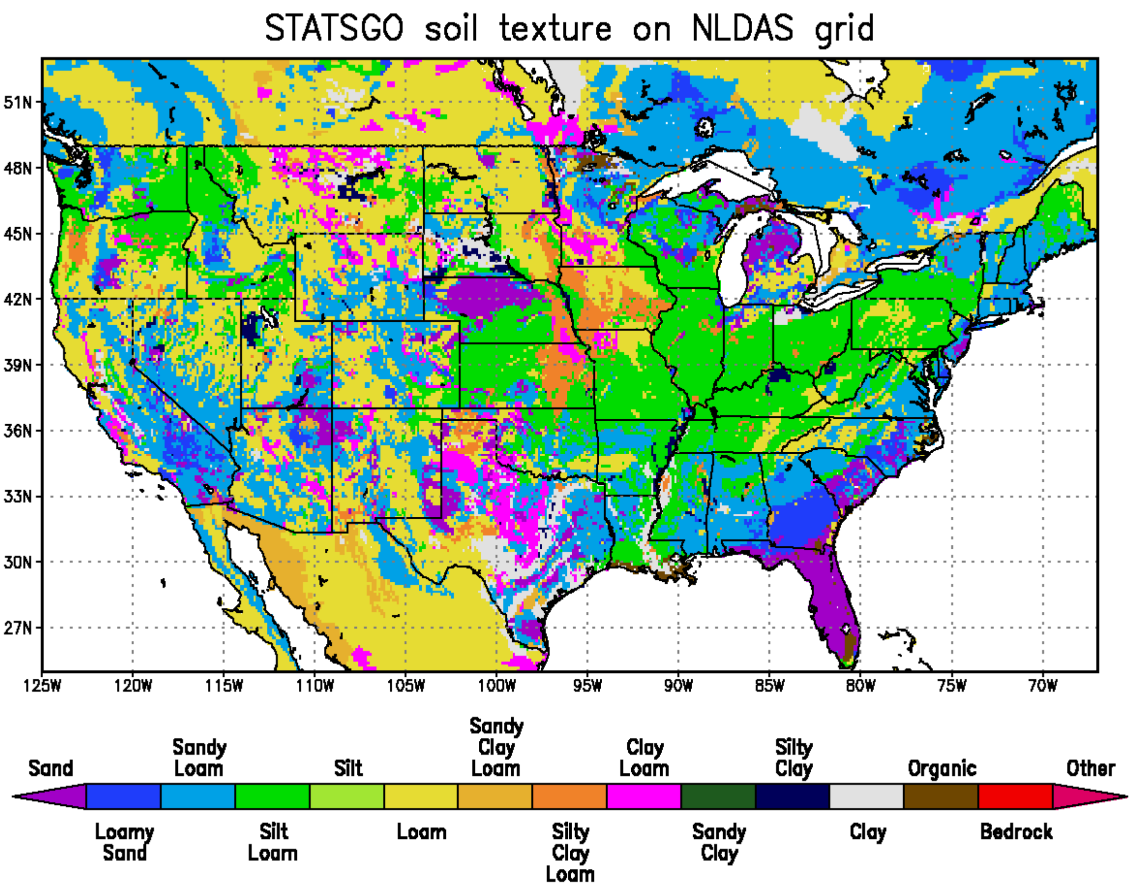

Fig. 3.1   Soil type nationally. Most of Florida, except for the NW panhandle is Sand while The NW panhandle is sandy loam.

First task was to locate the mesonet sites both in Florida and Oklahoma, the soil moisture data and stations rainfall data were extracted. The soil moisture and the rainfall data were plotted for each station for a full year. From that the maximum and minimum soil moisture was determined for all stations in each state. Then the rainfall at the station was also included in the plot. There was a strong correlation of when it rained a total of at least 0.5 inches in the last two days that the soil became saturated for all soil types. The soil remained saturated as long as that criteria was met. If it stopped raining the soil began to dry out about

10% each day and once it got to the minimum soil moisture, it remained at the minimum until it rained again.

3.1 Mesonet sites

The location of the mesonet sites that collect and record soil moisture data are illustrated in Figs. 3.1 and 3.2 for Oklahoma and Florida, respectively

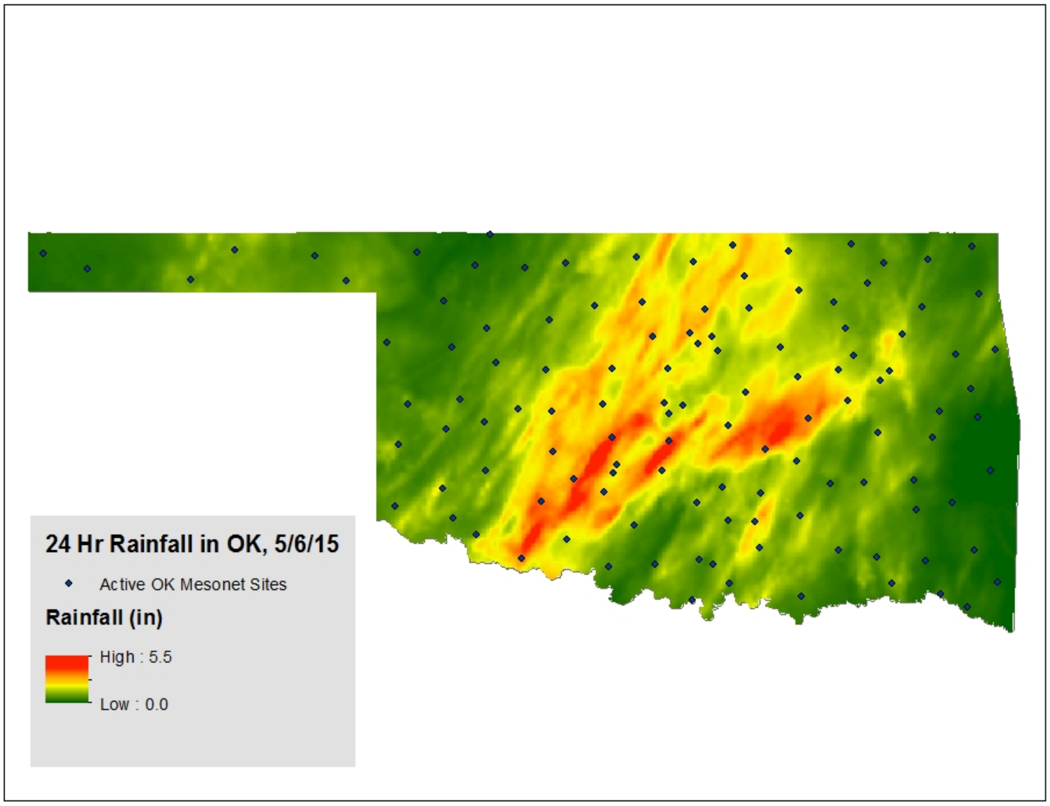

Fig. 3.2 Radar derived 24 hour rainfall over Oklahoma on 5/6/15. Locations of the Oklahoma mesonet sites are indicated by the black dots.

The above figure shows estimated rainfall in Oklahoma on May 6, 2015, derived from National Weather Service (NWS) radar estimates and then interpolated using the kriging function in ArcGIS. This rainfall event caused some flash flooding, especially in the central part of the state.

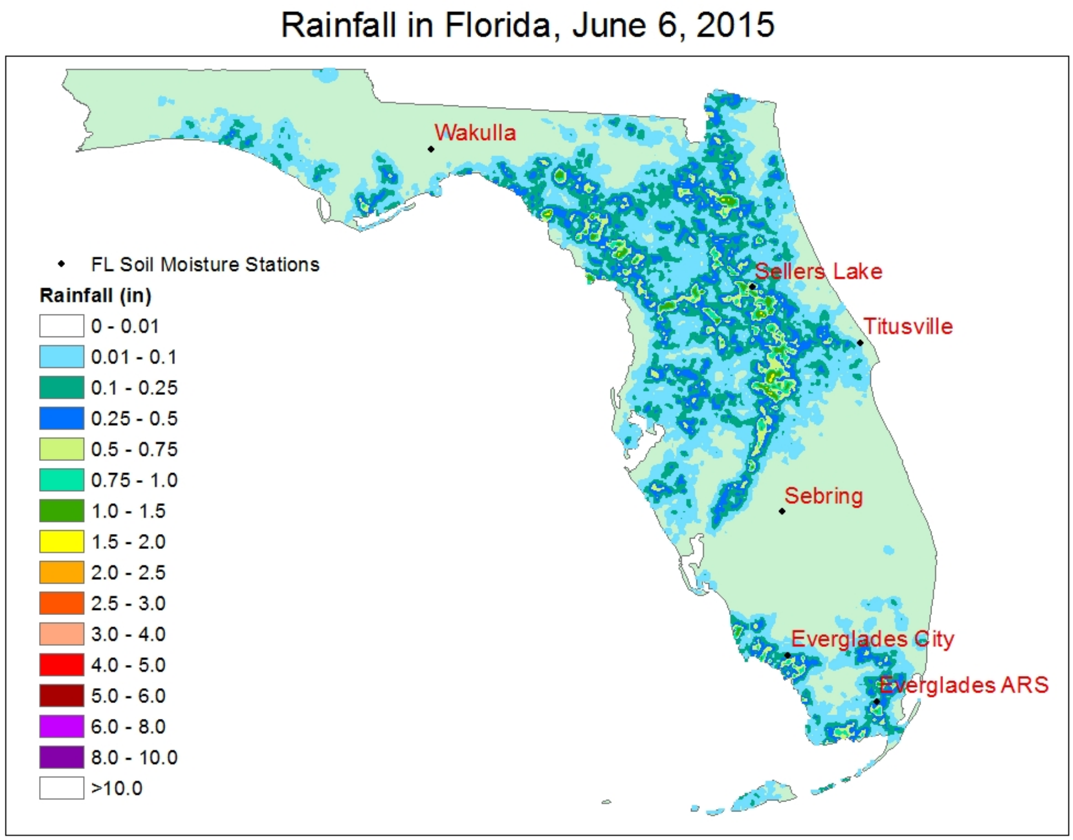

Fig. 3.2 Accumulated rainfall for June 6, 2015 across Florida. Location of surface mesonet sites that also measure rainfall and sole moisture are also indicated by name and location.

3.2 Soil type distribution

The type of soil for Oklahoma and Florida are given in Figure 3.3 Florida has a base of limestone over most of the land. The difference is fundamentally the depth of sand the overlies the limestone. The northern half of the panhandle has clay top instead of sand as it's formation was geologically different from the rest of Florida and it more nearly resembles the soil of Alabama and Georgia. One issue to consider is how the soil type might influence the retention and evaporation rate of soil moisture.

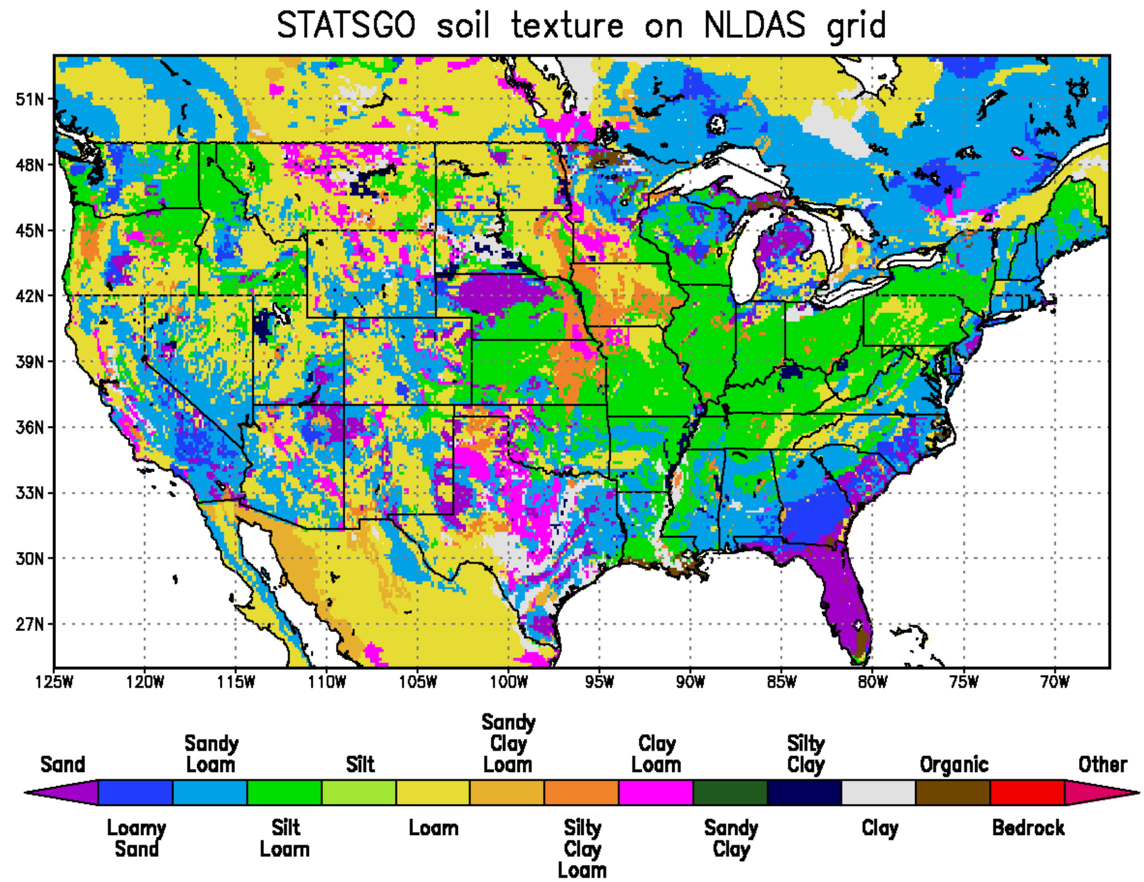

Fig. 3.3 Soil types for the United States.

4. RESULTS

4.1 Insitu measurements.

When it rain is porous soil, such as contains sufficient sand, percolates to lower levels. It is only when those lower levels become sufficiently saturated that the upper levels reflect the rainfall. Based on the data available here, that generally was about 0.5 inches of rain in a day. After that, until it rains sufficiently the soil dries out, either due to percolation, evaporation or some other means.

Oklahoma uses a effect of a heat impulse to derive the soil moisture. Florida measures the transmission of a 50 MHz pulse. So they each employ a different technology. It is not known how they compare. The Oklahoma sites are routinely calibrated by take a core sample of soil and weighting a cubic cm of soil at different depths. Then the soil sample is heated and dried and weighed again. The difference in weight is due to the loss of water. It is not known if or how the six stations (run by two different agencies) are calibrated. And examination of the data and the long period of outages, it is impossible to tell how well calibrated the data is and how well it is maintained. The character of the data gives little confidence that it is of any value and quantitatively it may be of no value in itself or as an instrument for calibration purposes. We simply had to ignore it as there was no indication that the data had any value at all.

We examined a year's worth of data. Even if there was reason to value the Florida data, because there are so few (6) stations in Florida that measure and report soil moisture, we went to Oklahoma that has the best mesonet in the country to develop and test an algorithm that could be applied in Florida and elsewhere. We examined at the soil moisture for each of the 86 stations and sought to find the maximum and minimum values. The distribution of stations and soil type was not uniform and we were prepared to deal with this. Since only the near surface soil is likely to be relevant in fog formation we restricted the analysis to the moisture at five centimeters depth. The soil moisture is presented as the fractional volume of water per volume of soil. Thus, the values are all numbers less than 1.0. There were no uniform range of values between soil types or even within the group of stations that were located on the same type of soil. The average maximum and average minimum value of soil moisture is shown in Fig. 4.1. The bar represents the average maximum and average minimum value for a particular group of stations of a particular soil type by the top and bottom of the blue rectangle. The number of stations represented in that soil type is indicated by the number in the blue box. The value of the maximum or minimum soil moisture in that group in indicated by the extension outside of the blue box. Although we treated each station by it's own maximum and minimum, a maximum of 0.33 cm^3 cm^{-3} and a minimum of 0.12 cm^3 cm^{-3} would be representative of nearly all the stations.

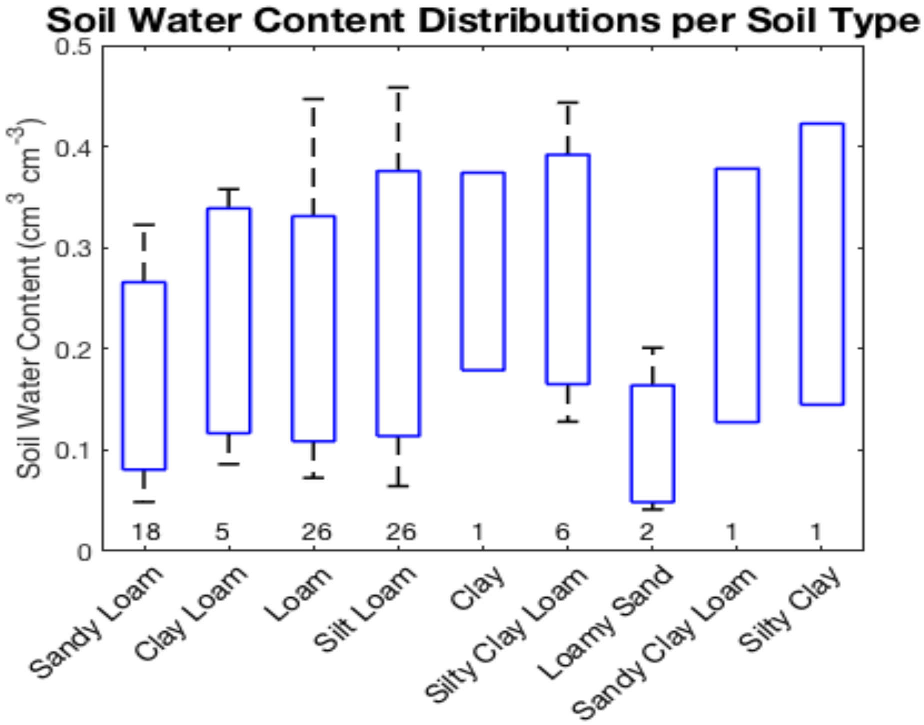

Fig. 4.1 Range of soil water content extremes for the Oklahoma stations.

Next we plotted the accumulated rainfall for the day when the soil moisture was reported. There exists a good correlation between the station measured rainfall and the soil moisture. During periods of no rain, the soil slowly dried out. This is illustrated by one (typical) station in Fig. 4.2. The red line is the fractional soil moisture. The solid green line represents the total rainfall data. The dashed green line represents the predicted accumulated soil moisture from the accumulated rainfall amount for that day. This is shown for May 6, 2015.

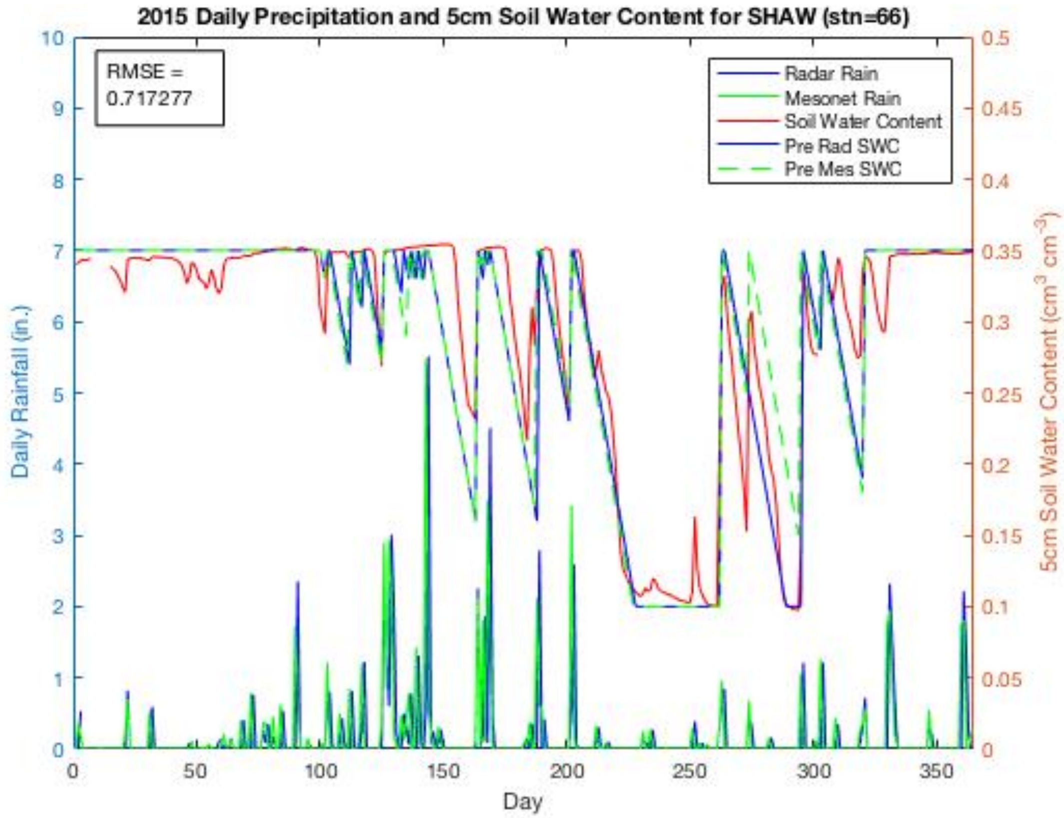

Fig. 4.2 Daily history of soil moisture for the station SHAW (station 66) for the year 2015. It is representative of the other 85 stations. The root mean square error is given in the box in the upper left and the legend is in the upper right. The ordinate values on the left are for the accumulated daily rainfall while the ordinate values on the right are the soil moisture values.

Applying this algorithm for all 86 stations will give a map of the soil moisture across Oklahoma. The panhandle is the driest region and the NE corner is where the soil is the wettest. For some stations, the cooler months the soil water content remained nearly saturated, regardless of the rainfall amount. Other stations showed a variation that was similar to the rest of the year. It is not clear what variables made it this way. The Oklahoma climate survey gives reason that the temperature was cooler and that retarded the evaporation and the evapotranspiration. It is not known if this is a regular occurrence or one that occurs occasionally. Further it is not known how site specific this effect is.

The Florida sites also show behavior in the cooler months that is seen the rest of the year. The Florida sites receive less attention than the Oklahoma sites and so it is less clear what the cause is. In a private communication it was relayed to us that the probed is placed in the top layer of the soil and that is was sand. With so few operational sites in Florida it is impossible to tell how representative these data are. They seem so suffer from inadequate maintenance.

4.2 Radar derived soil moisture

Again, since Florida does not measure soil moisture we have used the data from Oklahoma to calibrate rainfall rates with ensuing soil moisture. An example of the rainful for one day in Oklahoma is illustrated in the Fig. 3.2. Total rainfall is calculated from the rainfall rate as measured by the NWS radars. Typically the relationship is in the form

$$R = a \times Z^{b} \quad , \quad (1)$$

where **a** and **b** are know as a function of the type of convection. Z is the radar reflectivity factor. By integrating the rain-fall rate over time, the daily total rainfall is obtained.

After establishing that relationship, the rainfall at the station location was obtain from the NWS radar where they use the Z (Radar reflectivity factor, expressed in decibels) to R(rainfall) relationship as expressed in equation (1). The NWS provides a daily summary of total rainfall. It is important know the difference between the radar determined rainfall and the surface rain-gauge data. The gauge is a point measurement near where the soil probes were located. The radar data is from a volume that is on the order of one kilometer tall and wide and extending half a km horizontally and about one kilometer or more above the ground. These volumes are then averaged to proved a rainfall rate and integrated to provide the accumulated rainfall. It is this data that we seek to use to calculate the soil moisture on this much finer grid. Since the ground station data is much more dense in Oklahoma, it is the data from the Oklahoma mesonet that the procedure is tested and refined the rain/soil moisture algorithm for application in Florida and elsewhere.

To gain a better correlation between the radar estimate of rainfall and the gauge data we had to double the amount of suggested rainfall from the Z/R relationship. A modified Z/R relationship that was more appropriate for this application was created. By comparing the radar estimate with the rain gauge measurements at all the ground stations it was found that good agreement with the surface data was found by doubling the results from eq (1). This was true for all 86 statuibs. The results are shown in figure 4.2. Here the radar data is the blue line and the surface rain gauge data is green. Using the radar data alone, we then calculated the soil moisture for every day. Since the soil moisture drains or evaporates slowly, the effect of rain on soil is about a 10% depletion (by evaporation and drainage) every day when there is no rain. By contrast, when there is rain, the rise in soil moisture is immediate. The actual soil moisture as measured is given for every day of the year by the red line in Fig. 4.2. The calculated soil moisture based upon the on-site rain gauge is given by the dashed green line and the blue line is the soil moisture as determined by the radar data alone. The agreement was very good at all stations and for nearly every day of the year, the first 100 days being problematic (probably because of very cold weather) in many stations.

Similar plots for each station are presented in Appendix A. The overall agreement is excellent. The moisture values at each stations is as accurately determined by radar as by an on-site rain gauge. But the radar has 100 times better spatial resolution than even this dense rain-gauge network. The radar data is available through the NOAA/NWS.

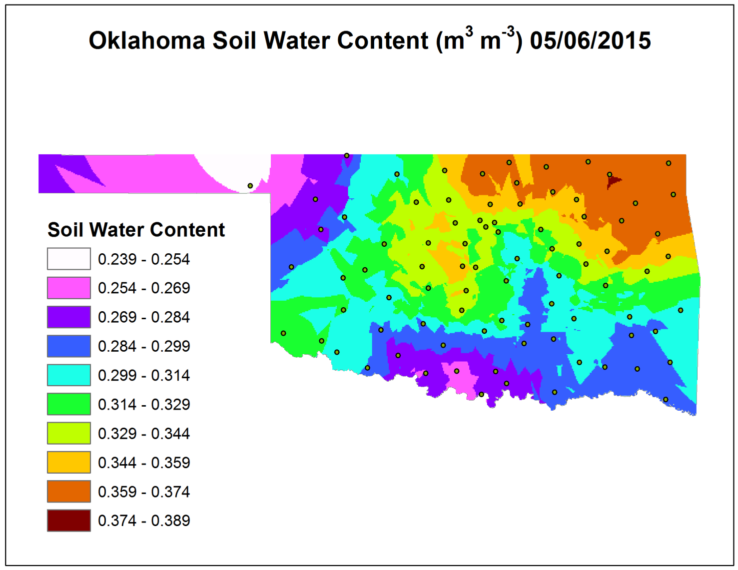

Fig. 4.3 Soil moisture as determined from the mesonet

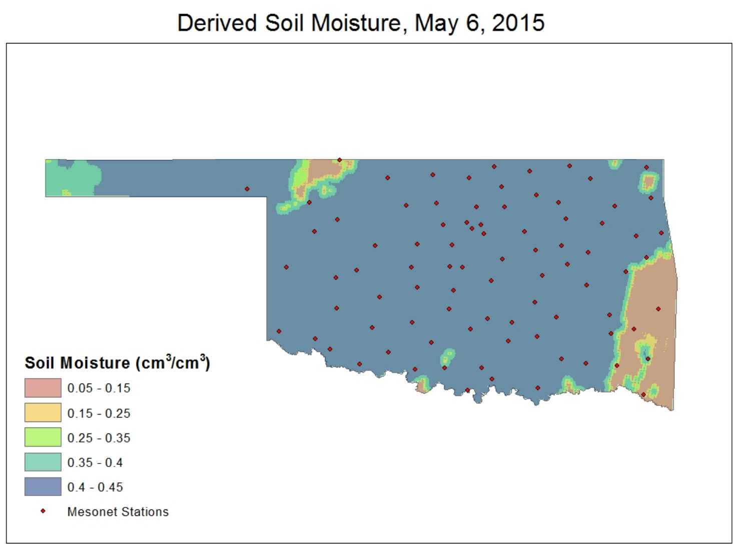

Fig. 4.4 Soil moisture as determined by the radar data.

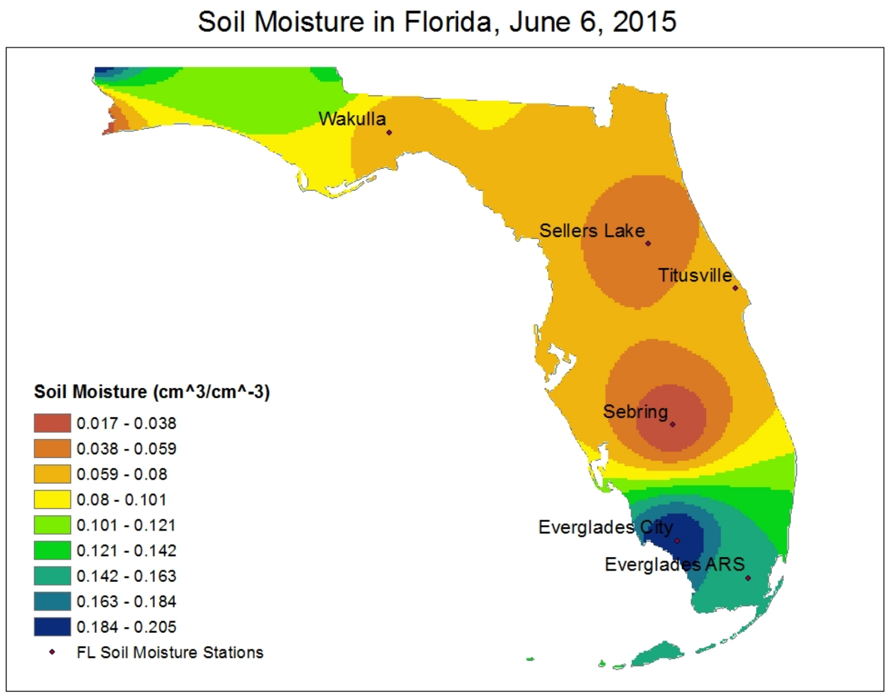

Fig. 4.5 Location of the 6 operational sites that provide soil moisture for Florida and soil moisture depicted for 6 June, 2015 from those 6 sites.

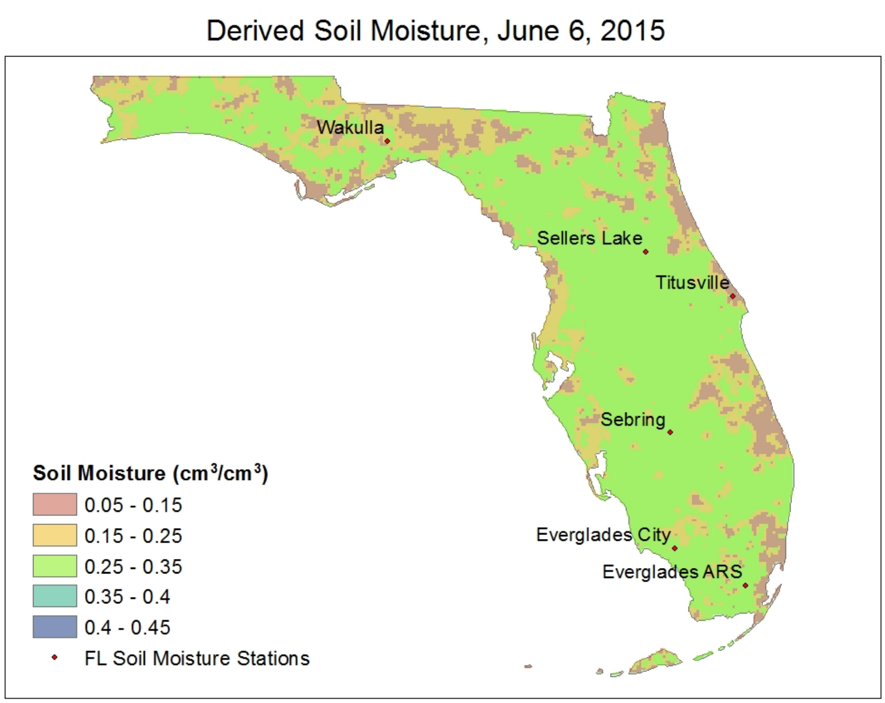

Fig. 4.6 Soil moisture derived from radar data. Note difference in scales from Fig 4.5.

Even with the dense ground station data from Oklahoma, the radar gives almost two orders of magnitude better spatial resolution. Thus, the soil moisture on the scale resolvable by the radar data for the same day (May 6, 2015) is shown Oklahoma in figure 4.3. The same comparison is available for Florida.

Satellites can estimate soil moisture in Oklahoma and Florida about once a day. The AMSR2 is an earth-orbiting satellite that takes its measurements of soil moisture over 99% of Earth over a period of two days. This method of microwave remote sensing of soil moisture is useful in that it allows for measurements to be taken at either night or day. The microwaves will not be affected by the atmosphere due to the earth's relative transparency to microwaves of longer wavelengths. Also, soil moisture parameters are easy to measure with a microwave sensor due to water's relatively high dielectric constant in the microwave band compared to that of the soil. To take into account the effects of vegetation, the sensor uses a correlation between optical thickness (τ_c) and the vegetation water content (W_c).

Satellites can estimate soil moisture in Oklahoma and Florida about once a day. The AMSR2 is an earth-orbiting satellite that takes its measurements of soil moisture over 99% of Earth over a period of two days. This method of microwave remote sensing of soil moisture is useful in that it allows for measurements to be taken at either night or day. The microwaves will not be affected by the atmosphere due to the earth's relative transparency to microwaves of longer wavelengths. Also, soil moisture parameters are easy to measure with a microwave sensor due to water's relatively high dielectric constant in the microwave band compared to that of the soil. To take into account the effects of vegetation, the sensor uses a correlation between optical thickness (τ_c) and the vegetation water content (W_c).

More information on the calibration techniques used for soil moisture retrieval for the AMSR2 can be found in Koiki (2013). While satellites can measure soil moisture, there is more processing involved and the results no better than using radar data, which requires very little processing.

5. SUMMARY

The role of soil moisture in the formation and maintenance of fog is unresolved. Arguments can be made for it inhibiting the formation and also how it might enhance the fog's formation. In general, the cooling effect is more likely to have a more dominate, albeit small effect in enhancing fog formation. It certainly is dominated by such condition such as week winds and high relative humidity. There is no doubt of the importance of the role of radiational cooling in the formation of radiation fog. In fact, Ray et. al (2015) presented a simple algorithm that did a credible job in forecasting the likely formation of fog and even its duration with a minor extension.

There are many problems with the direction measurement of soil moisture. The measurement may demonstrate time of relatively dry soil and moist soil, but quantitatively there is little evidence that they have much if any value. It is obviously a difficult measurement to take, but and periods of extreme values may be noted, but there is no evidence that any soil moisture measured in this study was quantitatively impressive. There were large gaps of missing data in almost all records. Florida only had a few stations where the data is recorded, and a visual inspection suggests that the see any value in the data at all.

What is promising is also many times less expensive and many time more accurate and many times more complete in its coverage. That is the use of NWS network radar data and the derived product of total daily rainfall to estimate soil moisture on nearly a four kilometer grid across the state. The results presented here show the much higher spatial resolution that is attainable and with comparable accuracy to any measured quantity. The data is free, and could be automatically processed and made available in its raw form and also imported into any boundary layer model. All this could be automated with very little maintenance. This is in spite of the fact that the radar pulse volume is typically a km above the ground and in the vertical plane covers much of the size of the cloud.

In summary:

1. Soil moisture is a second (or third) order effect. More significant is the (forecast) relative humidity and wind speed
2. Measurement of soil moisture is difficult and site specific and the results more qualitative than quantitate.
3. Soil type is not a strong determinate in the studies we preformed.
4. The use of radar to predict soil moisture is superior because
   a. It provides an equally accurate point (site specific) measurement of rainfall as a rain gauge.
   b. It provide orders of magnitude better spatial resolution of rainfall and therefore distribution of soil moisture.
5. Radar in combination with a suitable algorithm is much more economically feasible and in many cases with more accurate results.
6. The new Geostationary satellites (with vastly improved resolution) are superior for fog detection because of their vastly improved spatial resolution and their ability to have superior signal to noise ratio.
7. The Polar Orbiting satellites are superior for soil moisture detection because of they are the least expensive option and that they can measure soil moisture at a very high spatial resolution.
8. Soil moisture should be pursued by both Satellite measurement and Radar derived total rainfall. This analysis shows that the remote measurements are as accurate in determine soil moisture as *in situ* measurement.

REFERENCES

Bergot, Thierry, Daniel Guedalia, 1994: Numerical forecasting of radiation fog. Part I: Numerical model and sensitivity tests. *Mon. Wea. Rev.*, **122**, 1218–1230.

Bergot, Thierry, Dominique Carrer, Joël Noilhan, Philippe Bougeault, 2005: Improved site-specific numerical prediction of fog and low clouds: A feasibility study. *Wea. Forecasting*, **20**, 627–646.

Byers, H. R. (1959): General Meteorology. New York. McGraw-Hill. DOI 10.1002/qj.49708636716. 123pp.

Cermak, (2009): Beijing olympics as an aerosol field experiment. *Geophys. Res. Letters.* **36,** (10).

Court, A. and Gerston, R. (1966): Fog frequency in the United States. *Geographical Review*, Vol. 56, 543-560.

Croft, Paul J., Russell L. Pfost, Jeffrey M. Medlin, G. Alan Johnson, (1997): Fog Forecasting for the Southern Region: A conceptual model approach. *Wea. Forecasting*, **12**, 545–556.

d'Entremont, R. P., 1986: Low and midlevel cloud analysis using nighttime multispectral imagery. *J. Climate Appl. Meteor.*, 25, 1853–1869.

Duynkerke, P. G., 1991: Radiation fog: A comparison of model simulation with detailed observations. *Mon. Wea. Rev.*, 119, 324–34.

Ellrod et al. (1989) Elrod, G.P., and Lindstrom, 2006: Performance of satellite fog detection techniques With major, fog-related highway accidents. *Electronic Journal of Operational Meteorology* **2006-EJ3**

Ellrod G. P., (1995): Advances in the detection and analysis of fog at night using GOES multispectral infrared imager. *Wea. Forecasting.,* **10,** 606-619.

Eyre, J.R., J.L. Brownscombe, and R.J. Allam, (1984): Detection of fog at night using Advanced Resolution Radiometer (AVHRR) imagery. *Meteor. Mag.* **113,** 266-271.

Findlater, J., (1985): Field Investigations of radiation fog formation at outstations. *Meteor.Mag.*, **114,** 187-201.

Forthun, G. M., M.B. Johnson, W.G. Schmitz, J. Blume, and R.J. Caldwell, (2006): Trends in fog frequency and duration in the southeast United States**.** *Phys. Geography*, **27,** 206–222.

Hardwick, W.C. (1973) Monthly fog frequency in the continental United States. *Monthly Weather Review,* **101**, 763-766.

Hillger, D. W., (1999): GOES imager and sounder calibration, scaling and image quality. NOAA Tech. Rep. NESDIS 93, 34 pp.

Houghton, D. D., 1985: *Handbook of Meteorology*, 1st ed., John Wiley and Sons, 1461 pp.

Hunt, G. E. (1973): Radiative properties of terrestrial clouds at visible and infrared thermal window wavelengths. *Quart. J. Roy. Meteor. Soc.* **99,** 346-369.

Illston, B. G., J. B. Basara, and K. C. Crawford, (2004): Seasonal to internannual variationas of soil mositue measured in Oklahoma. *International J. of Climo.* **24**,1883-1896.

Illston, B. G., J. B. Basara, D. K. Fisher, R. Elliott, C. A. Fiebrich, K. C. Crawford, K. Humes, and E. Hunt, (2008): Mesoscale monitoring of soil moisture across a statewide network. *J. Atmos.and Ocean. Tech.* **24**, 167-182.

Koiki, T., 2013: Description of the GCOM-W1 AMSR2 soil moisture algorithm. *Descriptions of GCOM-W1 AMSR2 level 1R and level 2 algorithms*, Japan Aerospace Exploration Agency Earth Observation Research Center, 8-1–8-13.

Lavori, and Achtemier, G.L., (1995): A Fog and smoke risk index for estimating roadway visibility hazard. *National Wea. Digest.* **20** (1). 26-33.

Menzel, W. P. and J.F. W. Purdom, (1994): Introducing GOES-I: The first of a new generation of Geostationary Operational Environmental Satellites. *Bull. Amer. Meteor. Soc.* **75,** 757-781.

Montgomery, H. E. and L. W. Uccellini, (1985): VAS demonstration: (VISSR atmospheric sounder) description and final report. *NASA Reference Publication 1151.* National Aeronautics and Space Administration, 198 pp.

Peace, R. L., (1969): Heavy Fog Regions in the Conterminous United States. *Mon. Wea. Rev.* **97** (2) 116-123.

Ray, P. S., X. Du, and J. Rivard, (2013): Analysis of prospective systems for fog warnings. Florida Department of Transportation report number BDK83 997-19. 88 pp.

Ray P. S., and D. Lefran, (2015): Evaluation of fog predictions and detection. Florida Department of Transportation report number BDV30 997-30. 77 pp.

Stone, R, (1936): Fog in the United States and adjacent regions. *The Geographical Review*. **26** (1), 111-134,

Stull, R. B., 1999: *Meteorology for Scientists and Engineers* 2nd ed., Brooks/Cole, 502 pp.

Taylor, M. G. (1917): The formation of fog and mist. *Quarterly J. of the Royal Meteor. Soc.* **XLIII** (183).

Underwood, S. J., G. P., Ellrod, A.l. Kuhnert, (2004): A multiple-case analysis of nocturnal radiation-fog development off California utilizing GOES nighttime fog product. *J. Appl. Meteor.* **43,** 297-311.

Weinreb, M.P., M. Jamieson, N. Fulton, Y. Chen, J.X. Johnson, J. Bremer, C. Smith, and J. Baucom, (1997): Operational calibration of Geostationary Environmental Satellite-8 and -9 imagers and sounders," *Applied Optics*, **36**, pp. 6895-6904, 1997.

Willett, H. C., (1928): Fog and haze, their causes distribution and forecasting. *Mon. Wea. Rev.* **56** (11). 435- 468.

Appendix A

Soil moisture (red line), site measured rainfall (blue lines) and predicted soil moisture green line.

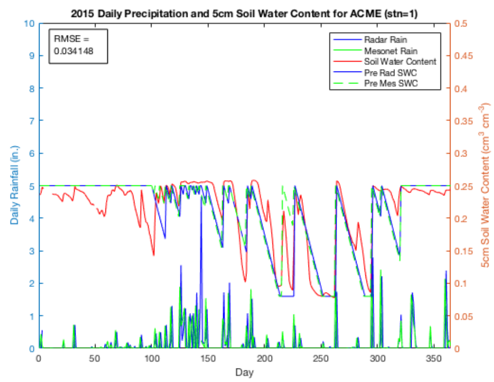
2015 Daily Precipitation and 5cm Soil Water Content for ACME (stn=1)
RMSE =
0.034148
Radar Rain
Mesonet Rain
Soil Water Content
Pre Rad SWC
Pre Mes SWC
Daily Rainfall (in.)
5cm Soil Water Content (cm^3 cm^{-3})
Day

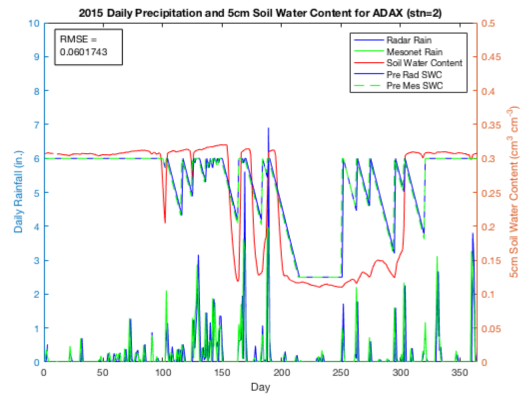
2015 Daily Precipitation and 5cm Soil Water Content for ADAX (stn=2)
RMSE =
0.0601743
Radar Rain
Mesonet Rain
Soil Water Content
Pre Rad SWC
Pre Mes SWC
Daily Rainfall (in.)
5cm Soil Water Content (cm^3 cm^{-3})
Day

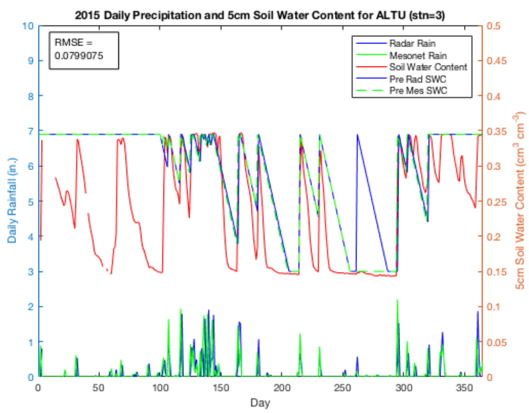
2015 Daily Precipitation and 5cm Soil Water Content for ALTU (stn=3)
RMSE =
0.0799075
Radar Rain
Mesonet Rain
Soil Water Content
Pre Rad SWC
Pre Mes SWC
Daily Rainfall (in.)
5cm Soil Water Content (cm^3 cm^{-3})
Day

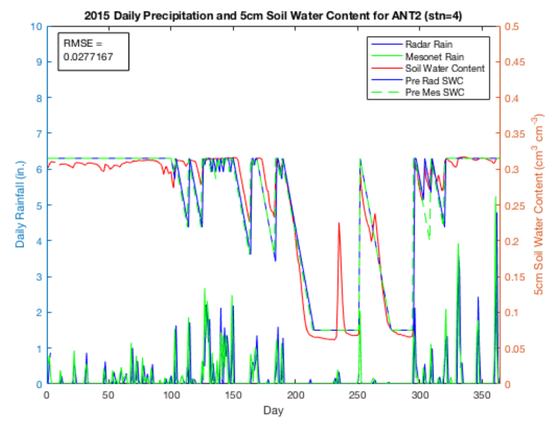
2015 Daily Precipitation and 5cm Soil Water Content for ANT2 (stn=4)
RMSE =
0.0277167
Radar Rain
Mesonet Rain
Soil Water Content
Pre Rad SWC
Pre Mes SWC
Daily Rainfall (in.)
5cm Soil Water Content (cm^3 cm^{-3})
Day

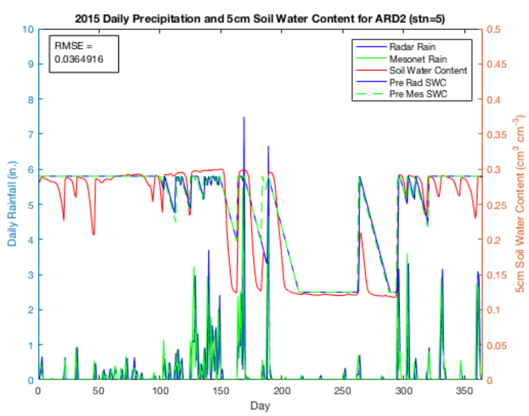
2015 Daily Precipitation and 5cm Soil Water Content for ARD2 (stn=5)
RMSE =
0.0364916
Radar Rain
Mesonet Rain
Soil Water Content
Pre Rad SWC
Pre Mes SWC
Daily Rainfall (in.)
5cm Soil Water Content (cm^3 cm^{-3})
Day

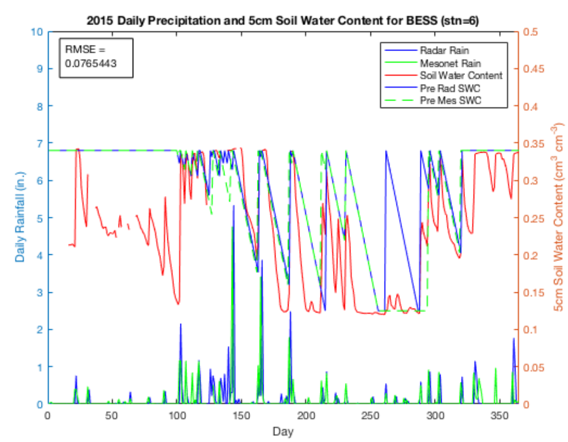
2015 Daily Precipitation and 5cm Soil Water Content for BESS (stn=6)
RMSE =
0.0765443
Radar Rain
Mesonet Rain
Soil Water Content
Pre Rad SWC
Pre Mes SWC
Daily Rainfall (in.)
5cm Soil Water Content (cm^3 cm^{-3})
Day

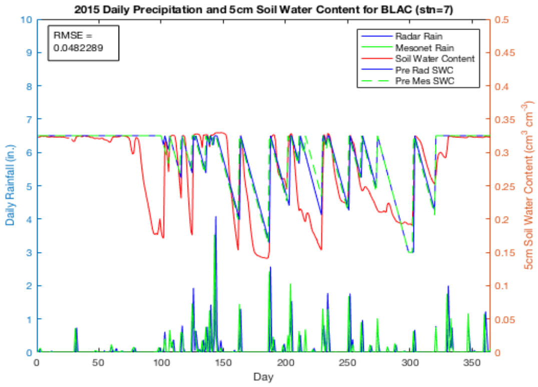
2015 Daily Precipitation and 5cm Soil Water Content for BLAC (stn=7)
RMSE =
0.0482289
Radar Rain
Mesonet Rain
Soil Water Content
Pre Rad SWC
Pre Mes SWC
Daily Rainfall (in.)
5cm Soil Water Content (cm3 cm-3)
Day

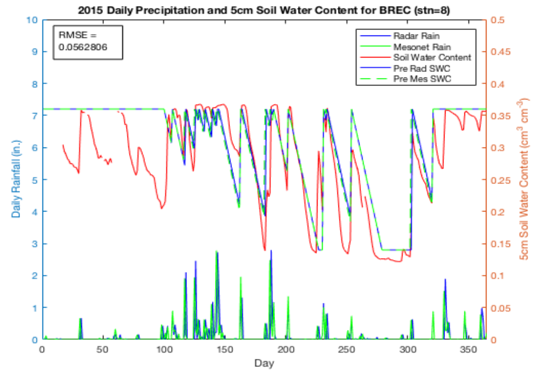
2015 Daily Precipitation and 5cm Soil Water Content for BREC (stn=8)
RMSE =
0.0562806
Radar Rain
Mesonet Rain
Soil Water Content
Pre Rad SWC
Pre Mes SWC
Daily Rainfall (in.)
5cm Soil Water Content (cm3 cm-3)
Day

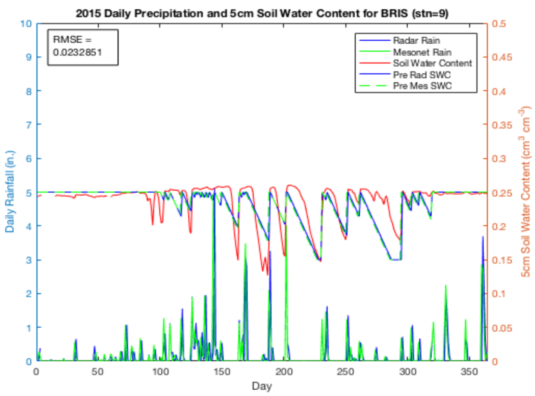
2015 Daily Precipitation and 5cm Soil Water Content for BRIS (stn=9)
RMSE =
0.0232851
Radar Rain
Mesonet Rain
Soil Water Content
Pre Rad SWC
Pre Mes SWC
Daily Rainfall (in.)
5cm Soil Water Content (cm3 cm-3)
Day

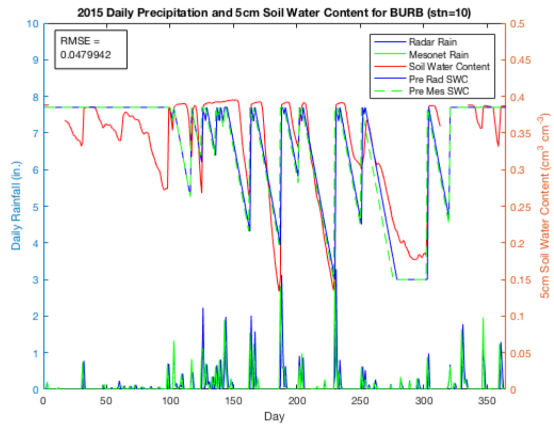
2015 Daily Precipitation and 5cm Soil Water Content for BURB (stn=10)
RMSE =
0.0479942
Radar Rain
Mesonet Rain
Soil Water Content
Pre Rad SWC
Pre Mes SWC
Daily Rainfall (in.)
5cm Soil Water Content (cm3 cm-3)
Day

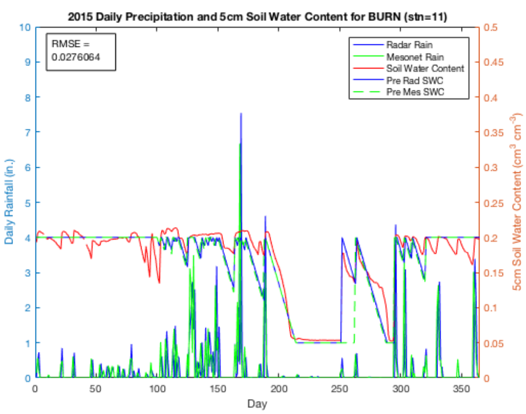
2015 Daily Precipitation and 5cm Soil Water Content for BURN (stn=11)
RMSE =
0.0276064
Radar Rain
Mesonet Rain
Soil Water Content
Pre Rad SWC
Pre Mes SWC
Daily Rainfall (in.)
5cm Soil Water Content (cm3 cm-3)
Day

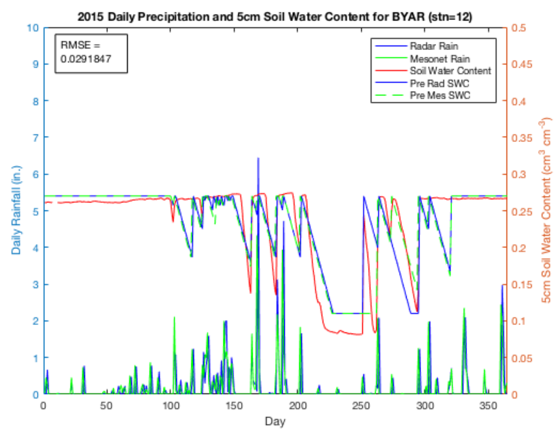
2015 Daily Precipitation and 5cm Soil Water Content for BYAR (stn=12)
RMSE =
0.0291847
Radar Rain
Mesonet Rain
Soil Water Content
Pre Rad SWC
Pre Mes SWC
Daily Rainfall (in.)
5cm Soil Water Content (cm3 cm-3)
Day

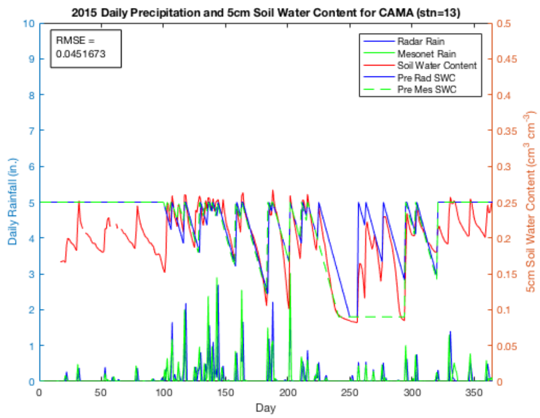
2015 Daily Precipitation and 5cm Soil Water Content for CAMA (stn=13)
RMSE = 0.0451673
Radar Rain
Mesonet Rain
Soil Water Content
Pre Rad SWC
Pre Mes SWC
Daily Rainfall (in.)
5cm Soil Water Content (cm³ cm⁻³)
Day

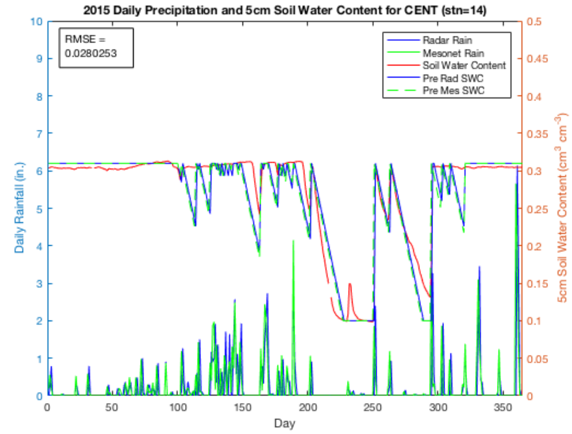
2015 Daily Precipitation and 5cm Soil Water Content for CENT (stn=14)
RMSE = 0.0280253
Radar Rain
Mesonet Rain
Soil Water Content
Pre Rad SWC
Pre Mes SWC
Daily Rainfall (in.)
5cm Soil Water Content (cm³ cm⁻³)
Day

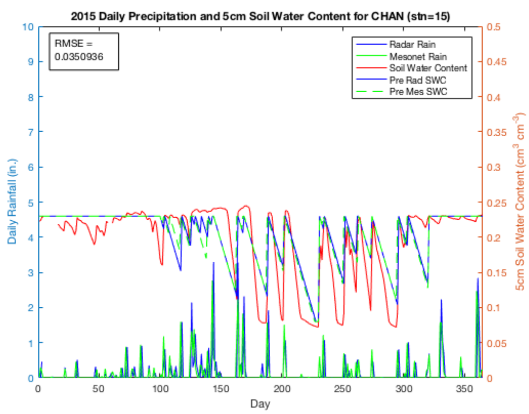
2015 Daily Precipitation and 5cm Soil Water Content for CHAN (stn=15)
RMSE = 0.0350936
Radar Rain
Mesonet Rain
Soil Water Content
Pre Rad SWC
Pre Mes SWC
Daily Rainfall (in.)
5cm Soil Water Content (cm³ cm⁻³)
Day

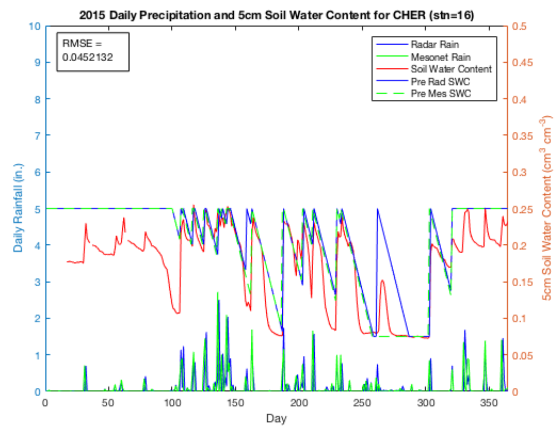
2015 Daily Precipitation and 5cm Soil Water Content for CHER (stn=16)
RMSE = 0.0452132
Radar Rain
Mesonet Rain
Soil Water Content
Pre Rad SWC
Pre Mes SWC
Daily Rainfall (in.)
5cm Soil Water Content (cm³ cm⁻³)
Day

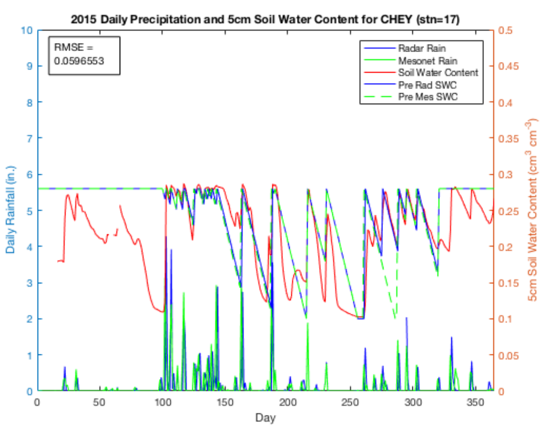
2015 Daily Precipitation and 5cm Soil Water Content for CHEY (stn=17)
RMSE = 0.0596553
Radar Rain
Mesonet Rain
Soil Water Content
Pre Rad SWC
Pre Mes SWC
Daily Rainfall (in.)
5cm Soil Water Content (cm³ cm⁻³)
Day

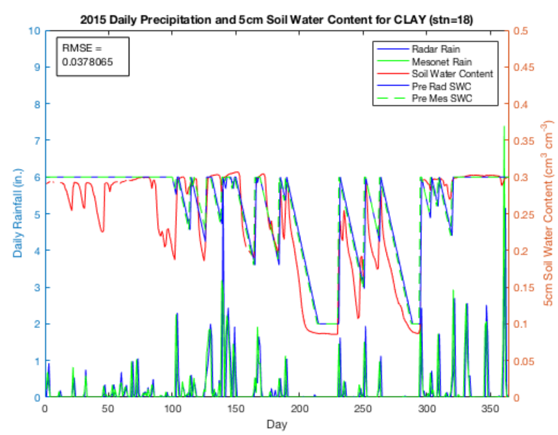
2015 Daily Precipitation and 5cm Soil Water Content for CLAY (stn=18)
RMSE = 0.0378065
Radar Rain
Mesonet Rain
Soil Water Content
Pre Rad SWC
Pre Mes SWC
Daily Rainfall (in.)
5cm Soil Water Content (cm³ cm⁻³)
Day

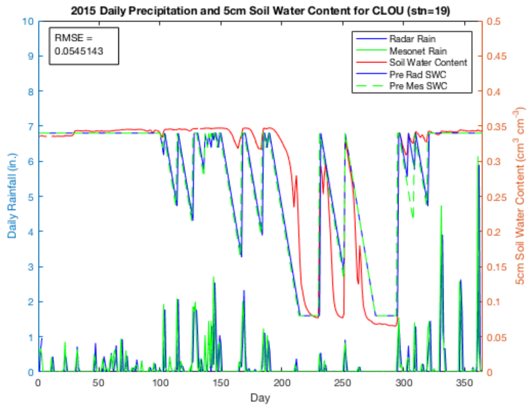
2015 Daily Precipitation and 5cm Soil Water Content for CLOU (stn=19)
RMSE =
0.0545143
Radar Rain
Mesonet Rain
Soil Water Content
Pre Rad SWC
Pre Mes SWC
Daily Rainfall (in.)
5cm Soil Water Content (cm^3 cm^{-3})
Day

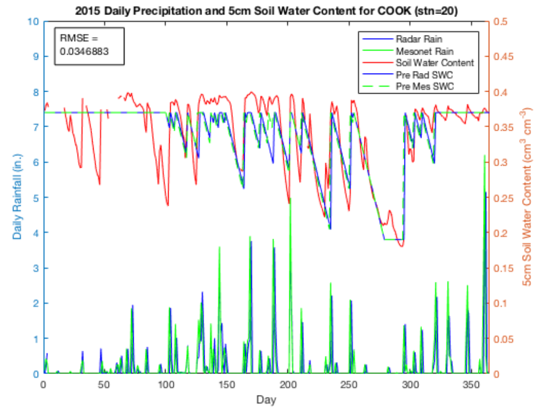
2015 Daily Precipitation and 5cm Soil Water Content for COOK (stn=20)
RMSE =
0.0346883
Radar Rain
Mesonet Rain
Soil Water Content
Pre Rad SWC
Pre Mes SWC
Daily Rainfall (in.)
5cm Soil Water Content (cm^3 cm^{-3})
Day

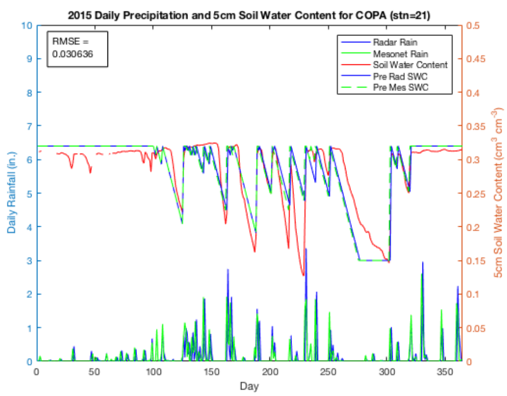
2015 Daily Precipitation and 5cm Soil Water Content for COPA (stn=21)
RMSE =
0.030636
Radar Rain
Mesonet Rain
Soil Water Content
Pre Rad SWC
Pre Mes SWC
Daily Rainfall (in.)
5cm Soil Water Content (cm^3 cm^{-3})
Day

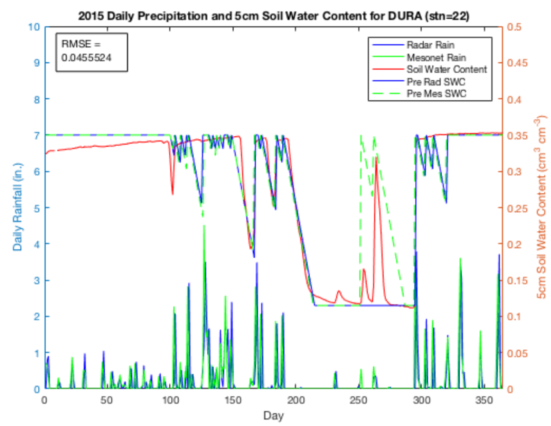
2015 Daily Precipitation and 5cm Soil Water Content for DURA (stn=22)
RMSE =
0.0455524
Radar Rain
Mesonet Rain
Soil Water Content
Pre Rad SWC
Pre Mes SWC
Daily Rainfall (in.)
5cm Soil Water Content (cm^3 cm^{-3})
Day

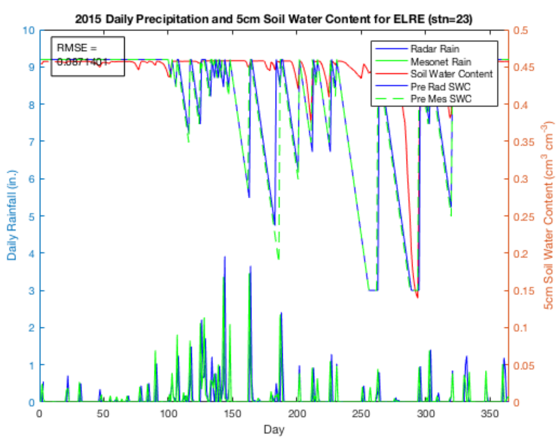
2015 Daily Precipitation and 5cm Soil Water Content for ELRE (stn=23)
RMSE =
0.0671401
Radar Rain
Mesonet Rain
Soil Water Content
Pre Rad SWC
Pre Mes SWC
Daily Rainfall (in.)
5cm Soil Water Content (cm^3 cm^{-3})
Day

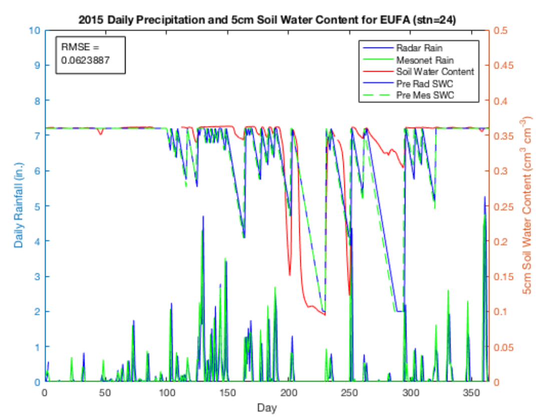
2015 Daily Precipitation and 5cm Soil Water Content for EUFA (stn=24)
RMSE =
0.0623887
Radar Rain
Mesonet Rain
Soil Water Content
Pre Rad SWC
Pre Mes SWC
Daily Rainfall (in.)
5cm Soil Water Content (cm^3 cm^{-3})
Day

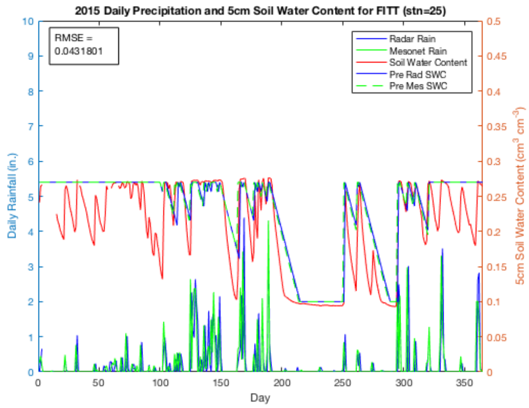
2015 Daily Precipitation and 5cm Soil Water Content for FITT (stn=25)
RMSE =
0.0431801
Radar Rain
Mesonet Rain
Soil Water Content
Pre Rad SWC
Pre Mes SWC
Daily Rainfall (in.)
5cm Soil Water Content (cm^3 cm^{-3})
Day

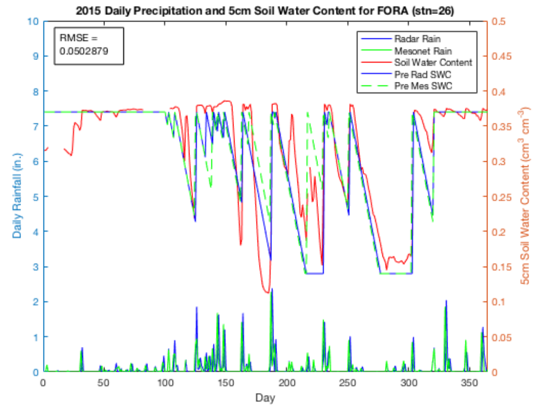
2015 Daily Precipitation and 5cm Soil Water Content for FORA (stn=26)
RMSE =
0.0502879
Radar Rain
Mesonet Rain
Soil Water Content
Pre Rad SWC
Pre Mes SWC
Daily Rainfall (in.)
5cm Soil Water Content (cm^3 cm^{-3})
Day

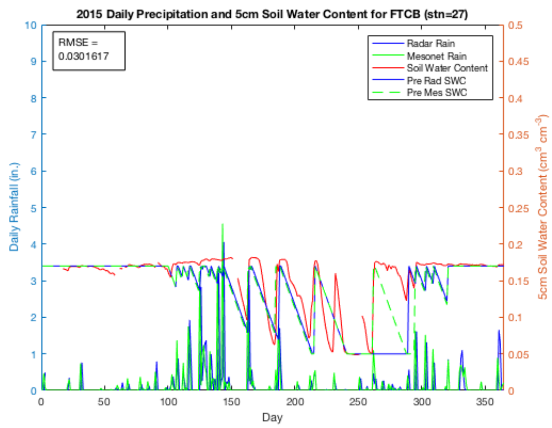
2015 Daily Precipitation and 5cm Soil Water Content for FTCB (stn=27)
RMSE =
0.0301617
Radar Rain
Mesonet Rain
Soil Water Content
Pre Rad SWC
Pre Mes SWC
Daily Rainfall (in.)
5cm Soil Water Content (cm^3 cm^{-3})
Day

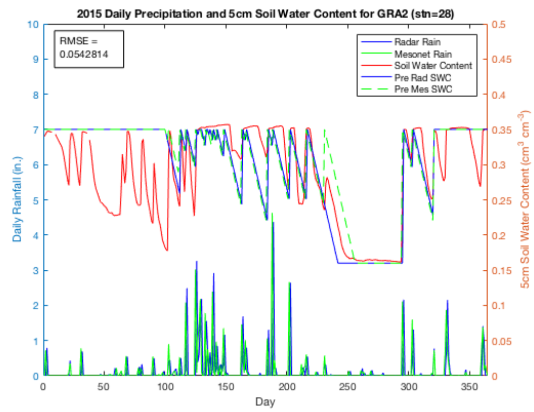
2015 Daily Precipitation and 5cm Soil Water Content for GRA2 (stn=28)
RMSE =
0.0542814
Radar Rain
Mesonet Rain
Soil Water Content
Pre Rad SWC
Pre Mes SWC
Daily Rainfall (in.)
5cm Soil Water Content (cm^3 cm^{-3})
Day

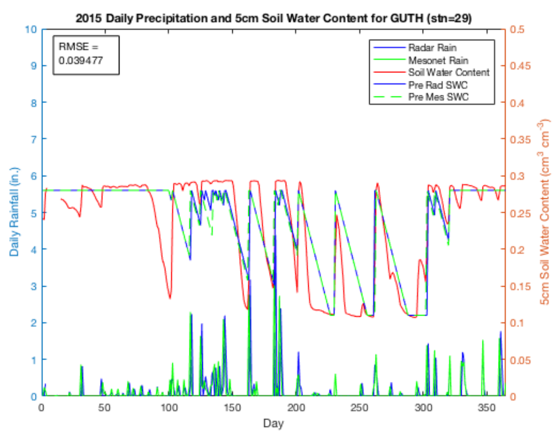
2015 Daily Precipitation and 5cm Soil Water Content for GUTH (stn=29)
RMSE =
0.039477
Radar Rain
Mesonet Rain
Soil Water Content
Pre Rad SWC
Pre Mes SWC
Daily Rainfall (in.)
5cm Soil Water Content (cm^3 cm^{-3})
Day

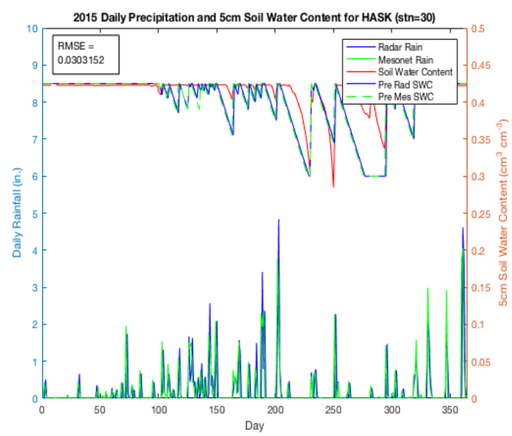
2015 Daily Precipitation and 5cm Soil Water Content for HASK (stn=30)
RMSE =
0.0303152
Radar Rain
Mesonet Rain
Soil Water Content
Pre Rad SWC
Pre Mes SWC
Daily Rainfall (in.)
5cm Soil Water Content (cm^3 cm^{-3})
Day

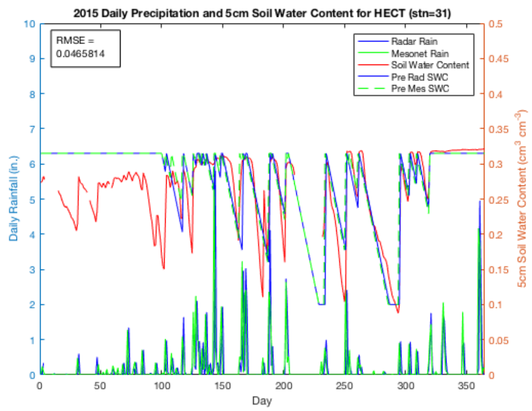
2015 Daily Precipitation and 5cm Soil Water Content for HECT (stn=31)
RMSE = 0.0465814
Radar Rain
Mesonet Rain
Soil Water Content
Pre Rad SWC
Pre Mes SWC
Daily Rainfall (in.)
5cm Soil Water Content (cm3 cm-3)
Day

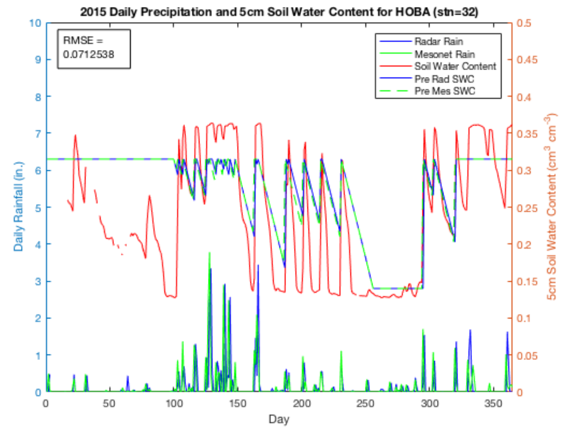
2015 Daily Precipitation and 5cm Soil Water Content for HOBA (stn=32)
RMSE = 0.0712538
Radar Rain
Mesonet Rain
Soil Water Content
Pre Rad SWC
Pre Mes SWC
Daily Rainfall (in.)
5cm Soil Water Content (cm3 cm-3)
Day

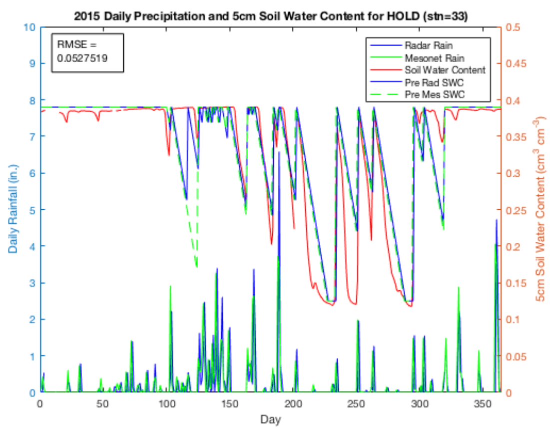
2015 Daily Precipitation and 5cm Soil Water Content for HOLD (stn=33)
RMSE = 0.0527519
Radar Rain
Mesonet Rain
Soil Water Content
Pre Rad SWC
Pre Mes SWC
Daily Rainfall (in.)
5cm Soil Water Content (cm3 cm-3)
Day

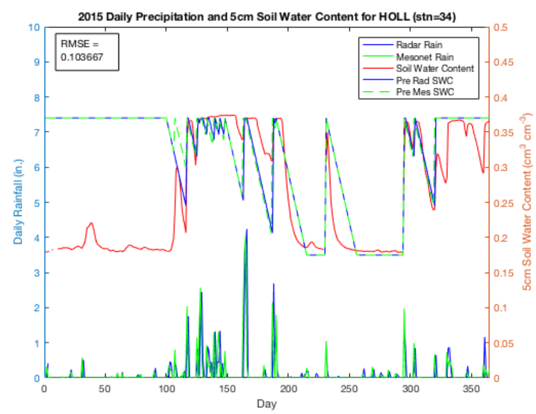
2015 Daily Precipitation and 5cm Soil Water Content for HOLL (stn=34)
RMSE = 0.103667
Radar Rain
Mesonet Rain
Soil Water Content
Pre Rad SWC
Pre Mes SWC
Daily Rainfall (in.)
5cm Soil Water Content (cm3 cm-3)
Day

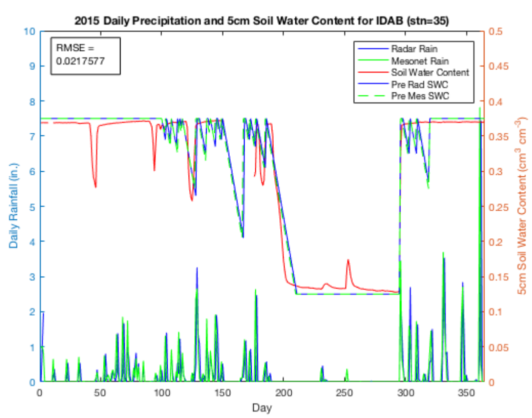
2015 Daily Precipitation and 5cm Soil Water Content for IDAB (stn=35)
RMSE = 0.0217577
Radar Rain
Mesonet Rain
Soil Water Content
Pre Rad SWC
Pre Mes SWC
Daily Rainfall (in.)
5cm Soil Water Content (cm3 cm-3)
Day

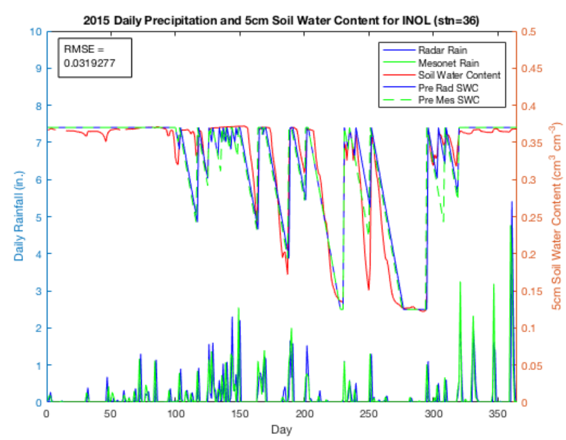
2015 Daily Precipitation and 5cm Soil Water Content for INOL (stn=36)
RMSE = 0.0319277
Radar Rain
Mesonet Rain
Soil Water Content
Pre Rad SWC
Pre Mes SWC
Daily Rainfall (in.)
5cm Soil Water Content (cm3 cm-3)
Day

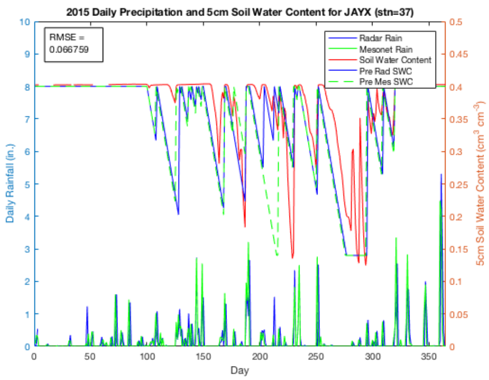
2015 Daily Precipitation and 5cm Soil Water Content for JAYX (stn=37)
RMSE =
0.066759
Radar Rain
Mesonet Rain
Soil Water Content
Pre Rad SWC
Pre Mes SWC
Daily Rainfall (in.)
5cm Soil Water Content (cm^3 cm^{-3})
Day

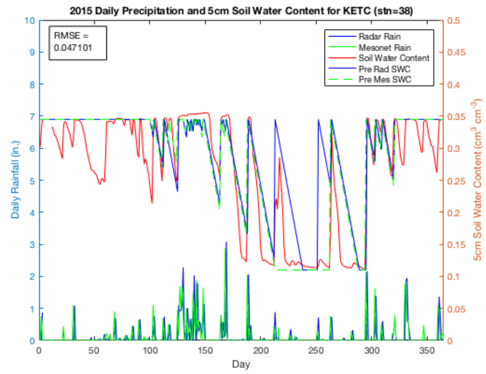
2015 Daily Precipitation and 5cm Soil Water Content for KETC (stn=38)
RMSE =
0.047101
Radar Rain
Mesonet Rain
Soil Water Content
Pre Rad SWC
Pre Mes SWC
Daily Rainfall (in.)
5cm Soil Water Content (cm^3 cm^{-3})
Day

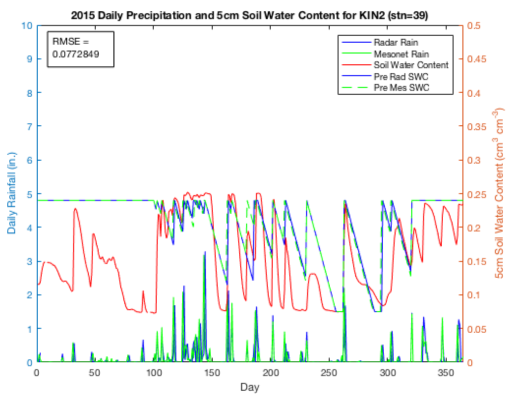
2015 Daily Precipitation and 5cm Soil Water Content for KIN2 (stn=39)
RMSE =
0.0772849
Radar Rain
Mesonet Rain
Soil Water Content
Pre Rad SWC
Pre Mes SWC
Daily Rainfall (in.)
5cm Soil Water Content (cm^3 cm^{-3})
Day

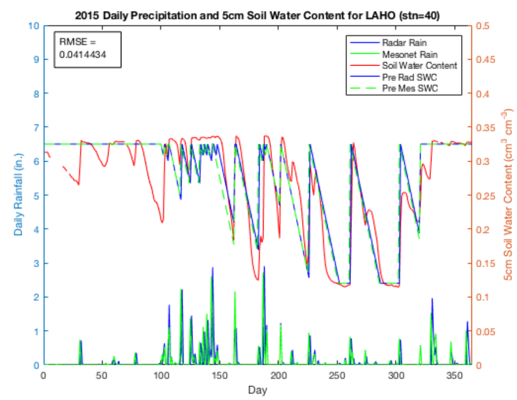
2015 Daily Precipitation and 5cm Soil Water Content for LAHO (stn=40)
RMSE =
0.0414434
Radar Rain
Mesonet Rain
Soil Water Content
Pre Rad SWC
Pre Mes SWC
Daily Rainfall (in.)
5cm Soil Water Content (cm^3 cm^{-3})
Day

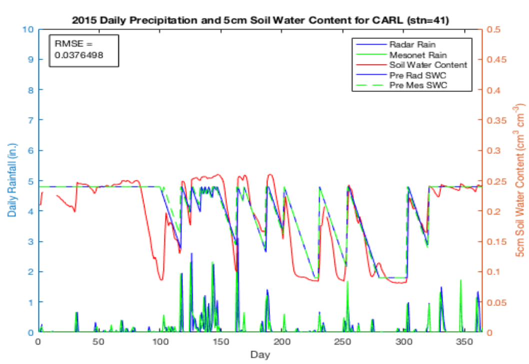
2015 Daily Precipitation and 5cm Soil Water Content for CARL (stn=41)
RMSE =
0.0376498
Radar Rain
Mesonet Rain
Soil Water Content
Pre Rad SWC
Pre Mes SWC
Daily Rainfall (in.)
5cm Soil Water Content (cm^3 cm^{-3})
Day

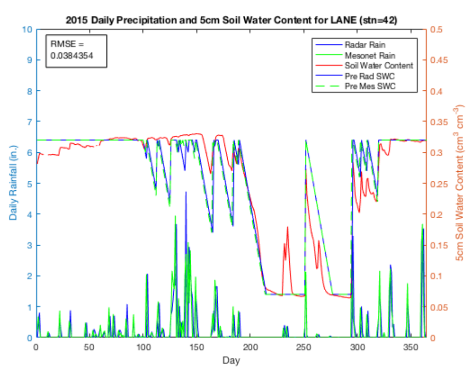
2015 Daily Precipitation and 5cm Soil Water Content for LANE (stn=42)
RMSE =
0.0384354
Radar Rain
Mesonet Rain
Soil Water Content
Pre Rad SWC
Pre Mes SWC
Daily Rainfall (in.)
5cm Soil Water Content (cm^3 cm^{-3})
Day

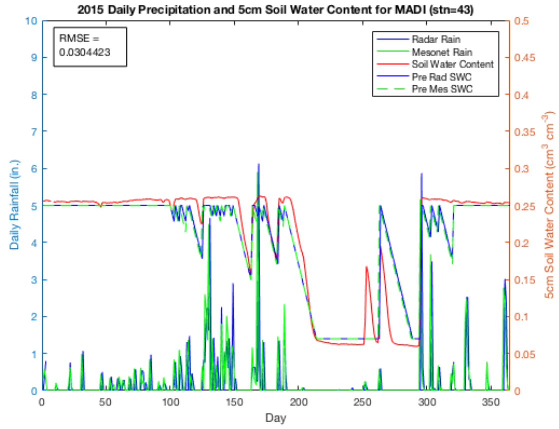
2015 Daily Precipitation and 5cm Soil Water Content for MADI (stn=43)
RMSE =
0.0304423
Radar Rain
Mesonet Rain
Soil Water Content
Pre Rad SWC
Pre Mes SWC
Daily Rainfall (in.)
5cm Soil Water Content (cm3 cm-3)
Day

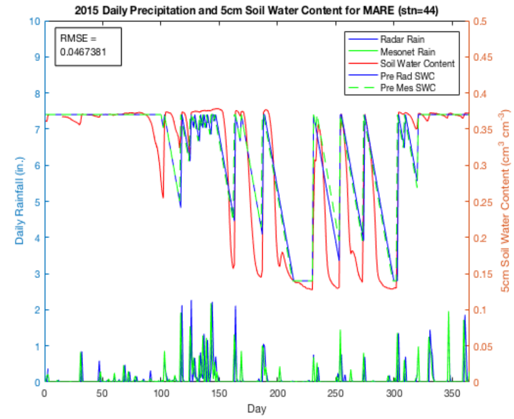
2015 Daily Precipitation and 5cm Soil Water Content for MARE (stn=44)
RMSE =
0.0467381
Radar Rain
Mesonet Rain
Soil Water Content
Pre Rad SWC
Pre Mes SWC
Daily Rainfall (in.)
5cm Soil Water Content (cm3 cm-3)
Day

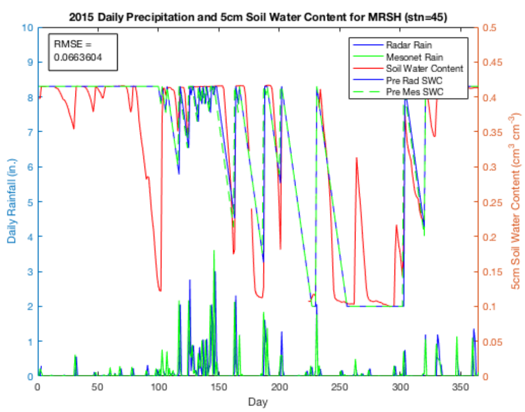
2015 Daily Precipitation and 5cm Soil Water Content for MRSH (stn=45)
RMSE =
0.0663604
Radar Rain
Mesonet Rain
Soil Water Content
Pre Rad SWC
Pre Mes SWC
Daily Rainfall (in.)
5cm Soil Water Content (cm3 cm-3)
Day

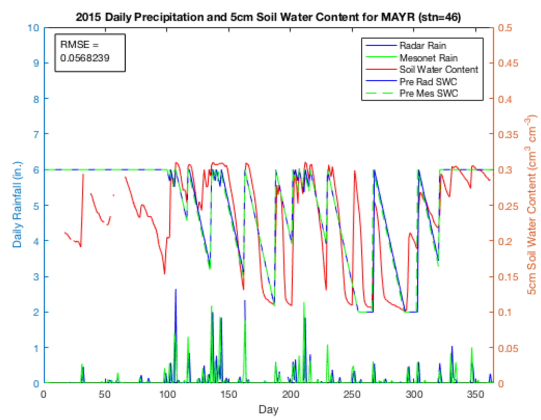
2015 Daily Precipitation and 5cm Soil Water Content for MAYR (stn=46)
RMSE =
0.0568239
Radar Rain
Mesonet Rain
Soil Water Content
Pre Rad SWC
Pre Mes SWC
Daily Rainfall (in.)
5cm Soil Water Content (cm3 cm-3)
Day

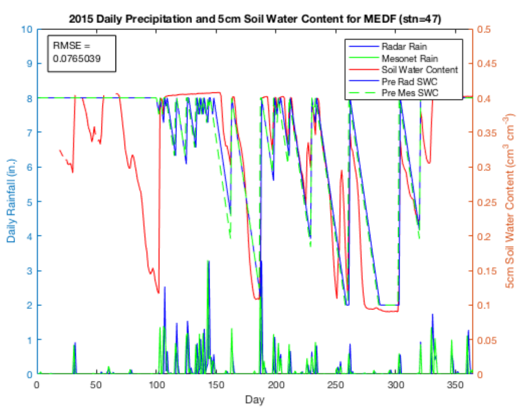
2015 Daily Precipitation and 5cm Soil Water Content for MEDF (stn=47)
RMSE =
0.0765039
Radar Rain
Mesonet Rain
Soil Water Content
Pre Rad SWC
Pre Mes SWC
Daily Rainfall (in.)
5cm Soil Water Content (cm3 cm-3)
Day

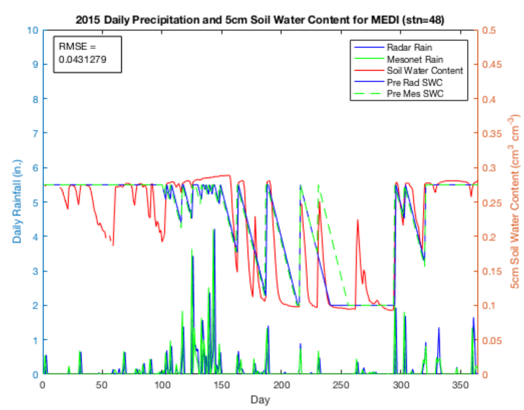
2015 Daily Precipitation and 5cm Soil Water Content for MEDI (stn=48)
RMSE =
0.0431279
Radar Rain
Mesonet Rain
Soil Water Content
Pre Rad SWC
Pre Mes SWC
Daily Rainfall (in.)
5cm Soil Water Content (cm3 cm-3)
Day

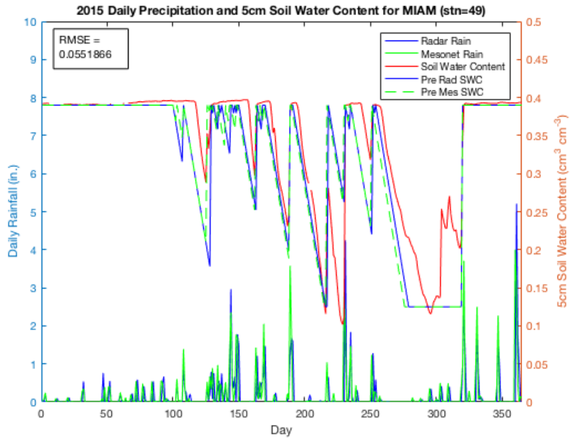
2015 Daily Precipitation and 5cm Soil Water Content for MIAM (stn=49)
RMSE =
0.0551866
Radar Rain
Mesonet Rain
Soil Water Content
Pre Rad SWC
Pre Mes SWC
Daily Rainfall (in.)
5cm Soil Water Content (cm^3 cm^{-3})
Day

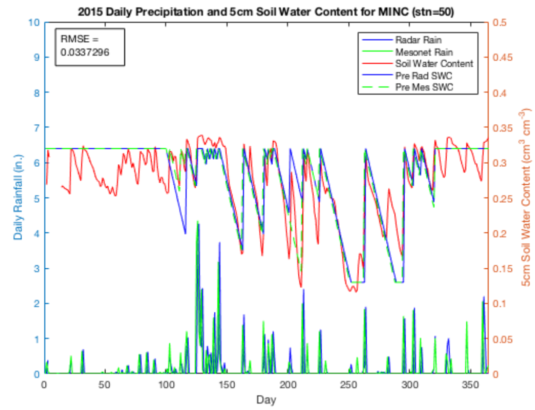
2015 Daily Precipitation and 5cm Soil Water Content for MINC (stn=50)
RMSE =
0.0337296
Radar Rain
Mesonet Rain
Soil Water Content
Pre Rad SWC
Pre Mes SWC
Daily Rainfall (in.)
5cm Soil Water Content (cm^3 cm^{-3})
Day

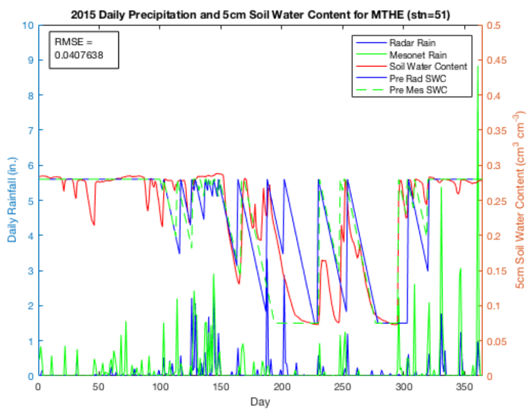
2015 Daily Precipitation and 5cm Soil Water Content for MTHE (stn=51)
RMSE =
0.0407638
Radar Rain
Mesonet Rain
Soil Water Content
Pre Rad SWC
Pre Mes SWC
Daily Rainfall (in.)
5cm Soil Water Content (cm^3 cm^{-3})
Day

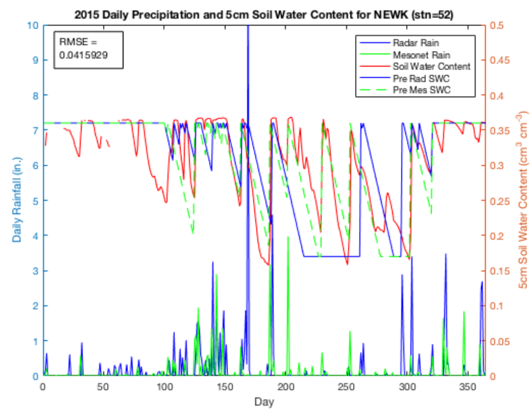
2015 Daily Precipitation and 5cm Soil Water Content for NEWK (stn=52)
RMSE =
0.0415929
Radar Rain
Mesonet Rain
Soil Water Content
Pre Rad SWC
Pre Mes SWC
Daily Rainfall (in.)
5cm Soil Water Content (cm^3 cm^{-3})
Day

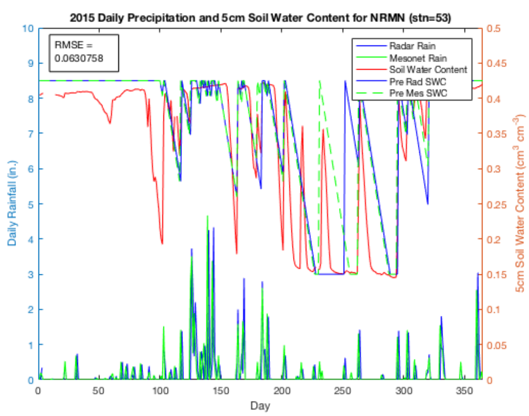
2015 Daily Precipitation and 5cm Soil Water Content for NRMN (stn=53)
RMSE =
0.0630758
Radar Rain
Mesonet Rain
Soil Water Content
Pre Rad SWC
Pre Mes SWC
Daily Rainfall (in.)
5cm Soil Water Content (cm^3 cm^{-3})
Day

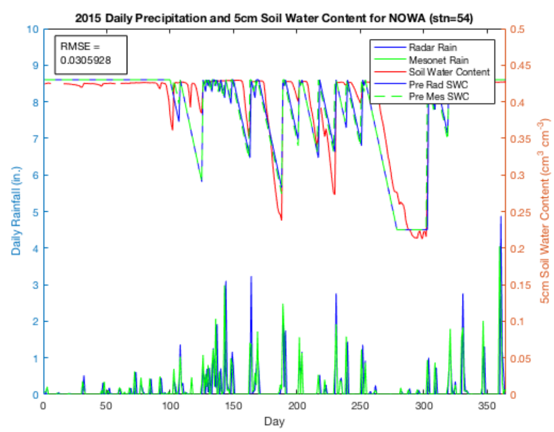
2015 Daily Precipitation and 5cm Soil Water Content for NOWA (stn=54)
RMSE =
0.0305928
Radar Rain
Mesonet Rain
Soil Water Content
Pre Rad SWC
Pre Mes SWC
Daily Rainfall (in.)
5cm Soil Water Content (cm^3 cm^{-3})
Day

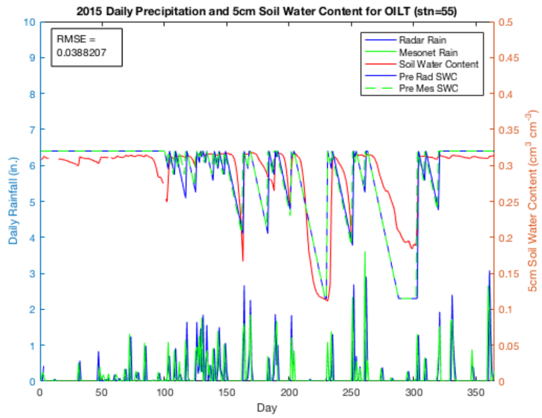
2015 Daily Precipitation and 5cm Soil Water Content for OILT (stn=55)
RMSE =
0.0388207
Radar Rain
Mesonet Rain
Soil Water Content
Pre Rad SWC
Pre Mes SWC
Daily Rainfall (in.)
5cm Soil Water Content (cm^3 cm^{-3})
Day

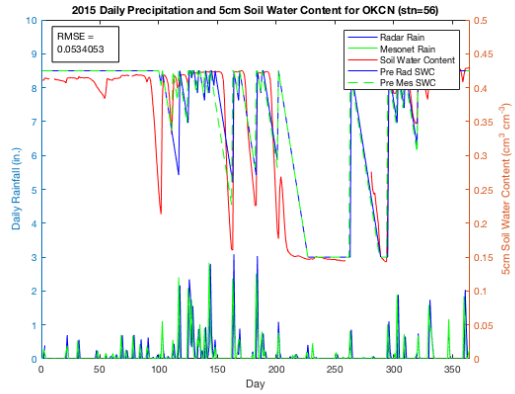
2015 Daily Precipitation and 5cm Soil Water Content for OKCN (stn=56)
RMSE =
0.0534053
Radar Rain
Mesonet Rain
Soil Water Content
Pre Rad SWC
Pre Mes SWC
Daily Rainfall (in.)
5cm Soil Water Content (cm^3 cm^{-3})
Day

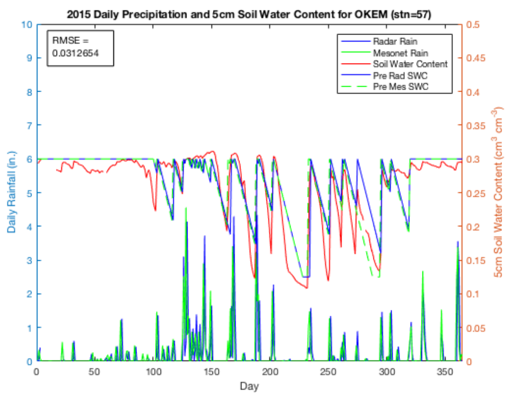
2015 Daily Precipitation and 5cm Soil Water Content for OKEM (stn=57)
RMSE =
0.0312654
Radar Rain
Mesonet Rain
Soil Water Content
Pre Rad SWC
Pre Mes SWC
Daily Rainfall (in.)
5cm Soil Water Content (cm^3 cm^{-3})
Day

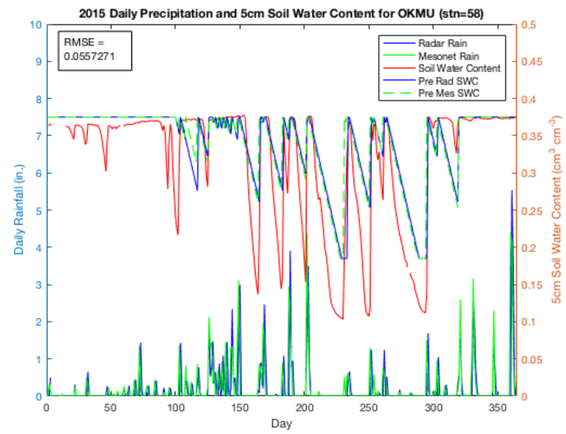
2015 Daily Precipitation and 5cm Soil Water Content for OKMU (stn=58)
RMSE =
0.0557271
Radar Rain
Mesonet Rain
Soil Water Content
Pre Rad SWC
Pre Mes SWC
Daily Rainfall (in.)
5cm Soil Water Content (cm^3 cm^{-3})
Day

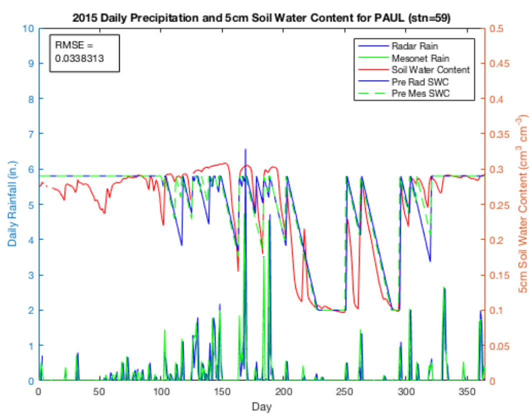
2015 Daily Precipitation and 5cm Soil Water Content for PAUL (stn=59)
RMSE =
0.0338313
Radar Rain
Mesonet Rain
Soil Water Content
Pre Rad SWC
Pre Mes SWC
Daily Rainfall (in.)
5cm Soil Water Content (cm^3 cm^{-3})
Day

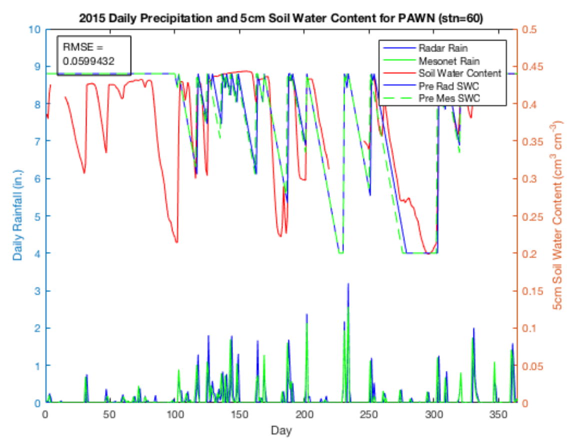
2015 Daily Precipitation and 5cm Soil Water Content for PAWN (stn=60)
RMSE =
0.0599432
Radar Rain
Mesonet Rain
Soil Water Content
Pre Rad SWC
Pre Mes SWC
Daily Rainfall (in.)
5cm Soil Water Content (cm^3 cm^{-3})
Day

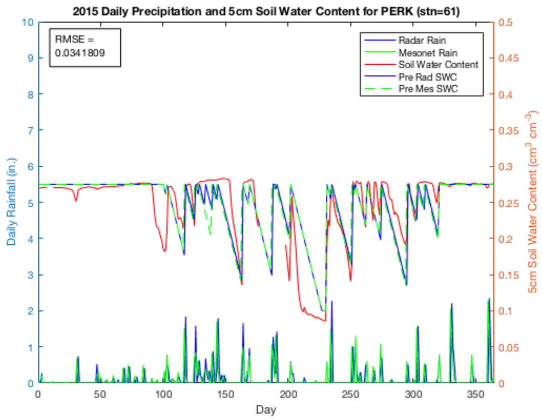
2015 Daily Precipitation and 5cm Soil Water Content for PERK (stn=61)
RMSE =
0.0341809
Radar Rain
Mesonet Rain
Soil Water Content
Pre Rad SWC
Pre Mes SWC
Daily Rainfall (in.)
5cm Soil Water Content (cm^3 cm^{-3})
Day

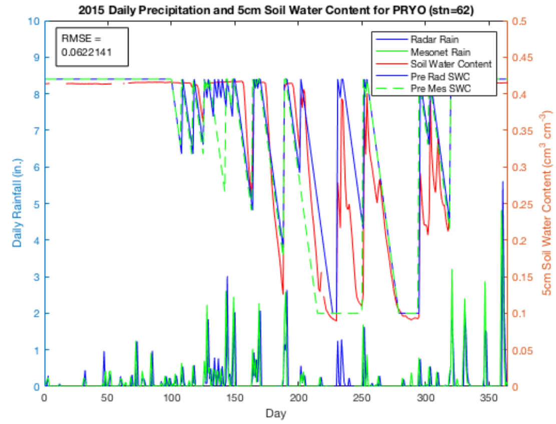
2015 Daily Precipitation and 5cm Soil Water Content for PRYO (stn=62)
RMSE =
0.0622141
Radar Rain
Mesonet Rain
Soil Water Content
Pre Rad SWC
Pre Mes SWC
Daily Rainfall (in.)
5cm Soil Water Content (cm^3 cm^{-3})
Day

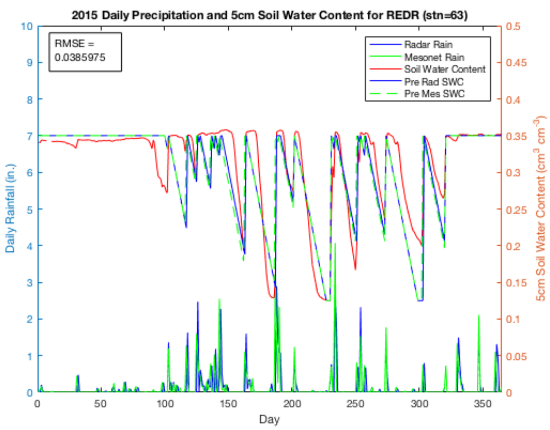
2015 Daily Precipitation and 5cm Soil Water Content for REDR (stn=63)
RMSE =
0.0385975
Radar Rain
Mesonet Rain
Soil Water Content
Pre Rad SWC
Pre Mes SWC
Daily Rainfall (in.)
5cm Soil Water Content (cm^3 cm^{-3})
Day

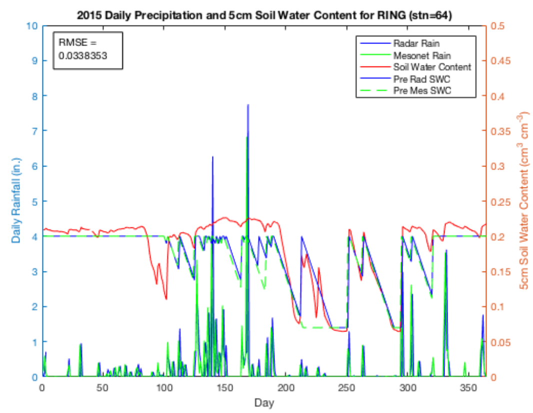
2015 Daily Precipitation and 5cm Soil Water Content for RING (stn=64)
RMSE =
0.0338353
Radar Rain
Mesonet Rain
Soil Water Content
Pre Rad SWC
Pre Mes SWC
Daily Rainfall (in.)
5cm Soil Water Content (cm^3 cm^{-3})
Day

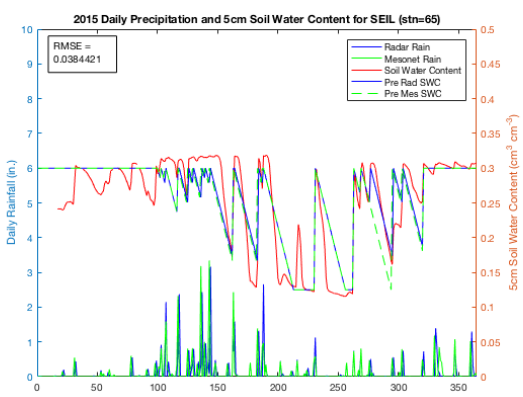
2015 Daily Precipitation and 5cm Soil Water Content for SEIL (stn=65)
RMSE =
0.0384421
Radar Rain
Mesonet Rain
Soil Water Content
Pre Rad SWC
Pre Mes SWC
Daily Rainfall (in.)
5cm Soil Water Content (cm^3 cm^{-3})
Day

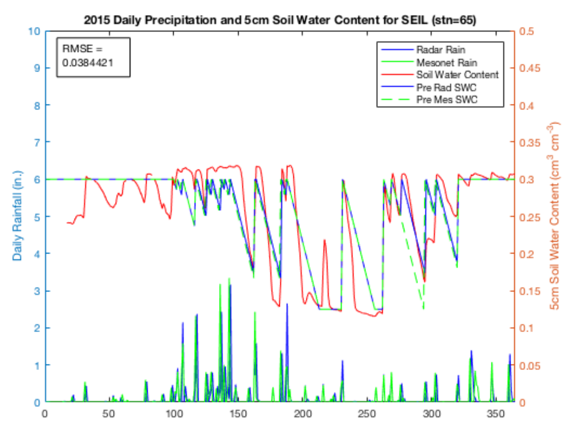
2015 Daily Precipitation and 5cm Soil Water Content for SEIL (stn=65)
RMSE =
0.0384421
Radar Rain
Mesonet Rain
Soil Water Content
Pre Rad SWC
Pre Mes SWC
Daily Rainfall (in.)
5cm Soil Water Content (cm^3 cm^{-3})
Day

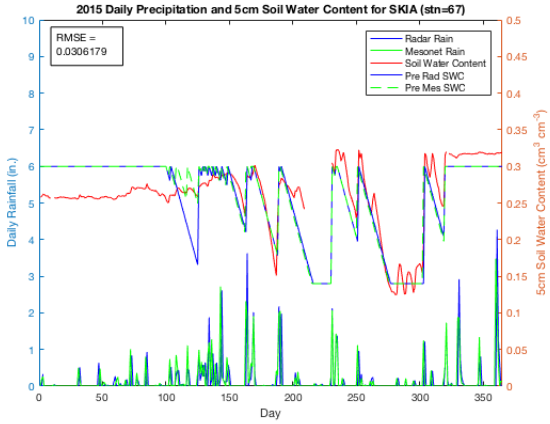
2015 Daily Precipitation and 5cm Soil Water Content for SKIA (stn=67)
RMSE =
0.0306179
Radar Rain
Mesonet Rain
Soil Water Content
Pre Rad SWC
Pre Mes SWC
Daily Rainfall (in.)
5cm Soil Water Content (cm^3 cm^{-3})
Day

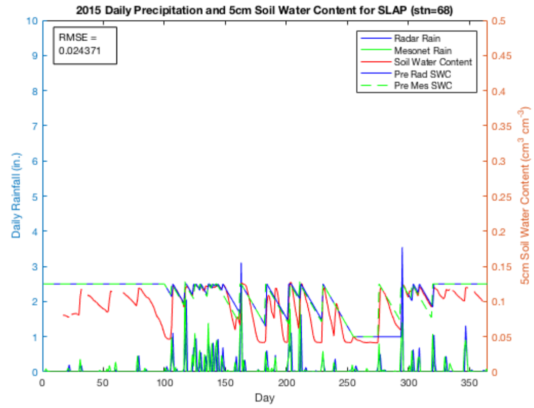
2015 Daily Precipitation and 5cm Soil Water Content for SLAP (stn=68)
RMSE =
0.024371
Radar Rain
Mesonet Rain
Soil Water Content
Pre Rad SWC
Pre Mes SWC
Daily Rainfall (in.)
5cm Soil Water Content (cm^3 cm^{-3})
Day

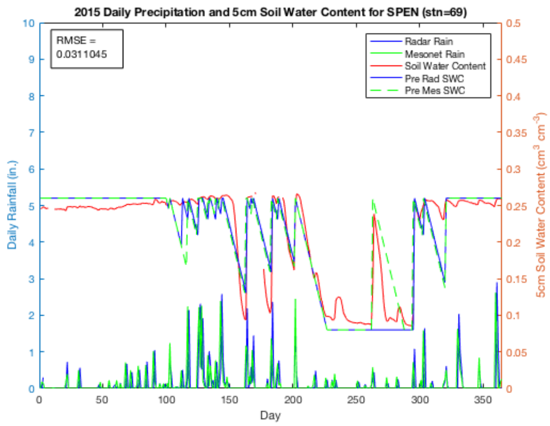
2015 Daily Precipitation and 5cm Soil Water Content for SPEN (stn=69)
RMSE =
0.0311045
Radar Rain
Mesonet Rain
Soil Water Content
Pre Rad SWC
Pre Mes SWC
Daily Rainfall (in.)
5cm Soil Water Content (cm^3 cm^{-3})
Day

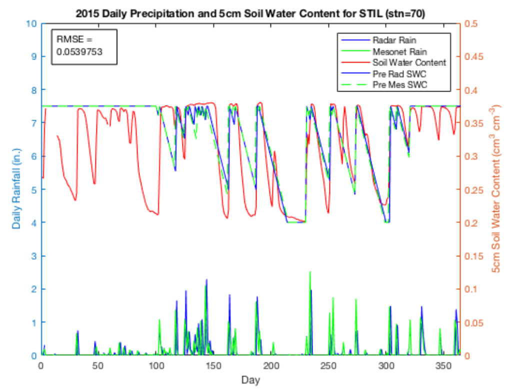
2015 Daily Precipitation and 5cm Soil Water Content for STIL (stn=70)
RMSE =
0.0539753
Radar Rain
Mesonet Rain
Soil Water Content
Pre Rad SWC
Pre Mes SWC
Daily Rainfall (in.)
5cm Soil Water Content (cm^3 cm^{-3})
Day

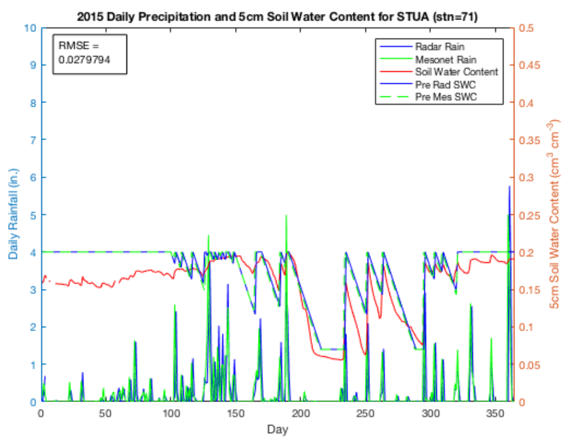
2015 Daily Precipitation and 5cm Soil Water Content for STUA (stn=71)
RMSE =
0.0279794
Radar Rain
Mesonet Rain
Soil Water Content
Pre Rad SWC
Pre Mes SWC
Daily Rainfall (in.)
5cm Soil Water Content (cm^3 cm^{-3})
Day

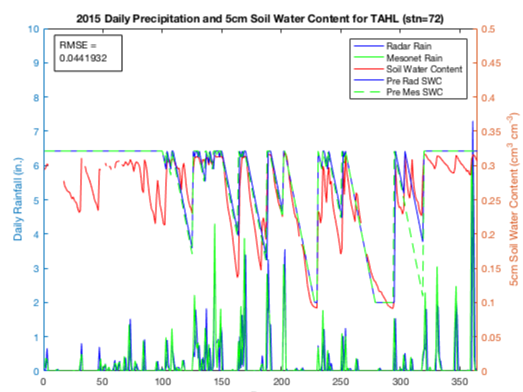
2015 Daily Precipitation and 5cm Soil Water Content for TAHL (stn=72)
RMSE =
0.0441932
Radar Rain
Mesonet Rain
Soil Water Content
Pre Rad SWC
Pre Mes SWC
Daily Rainfall (in.)
5cm Soil Water Content (cm^3 cm^{-3})
Day

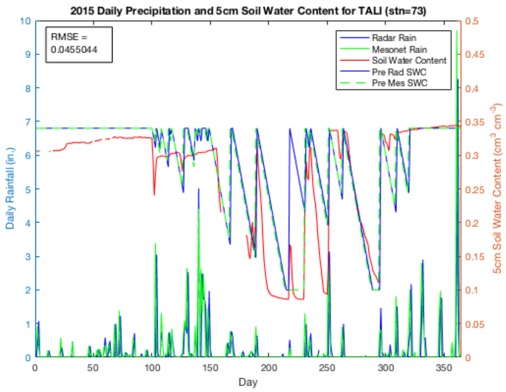
2015 Daily Precipitation and 5cm Soil Water Content for TALI (stn=73)
RMSE =
0.0455044
Radar Rain
Mesonet Rain
Soil Water Content
Pre Rad SWC
Pre Mes SWC
Daily Rainfall (in.)
5cm Soil Water Content (cm³ cm⁻³)
Day

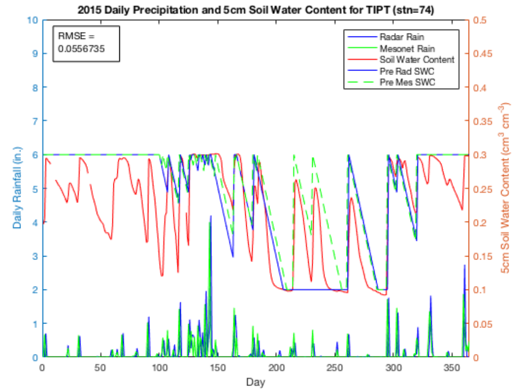
2015 Daily Precipitation and 5cm Soil Water Content for TIPT (stn=74)
RMSE =
0.0556735
Radar Rain
Mesonet Rain
Soil Water Content
Pre Rad SWC
Pre Mes SWC
Daily Rainfall (in.)
5cm Soil Water Content (cm³ cm⁻³)
Day

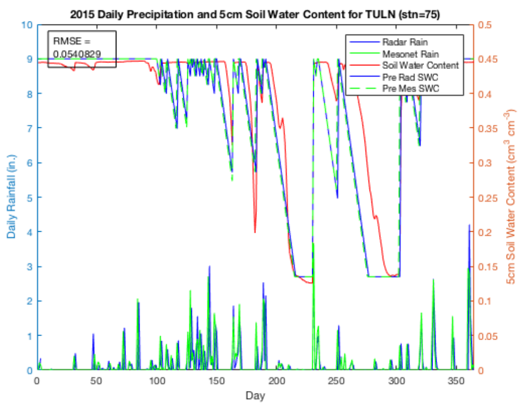
2015 Daily Precipitation and 5cm Soil Water Content for TULN (stn=75)
RMSE =
0.0540829
Radar Rain
Mesonet Rain
Soil Water Content
Pre Rad SWC
Pre Mes SWC
Daily Rainfall (in.)
5cm Soil Water Content (cm³ cm⁻³)
Day

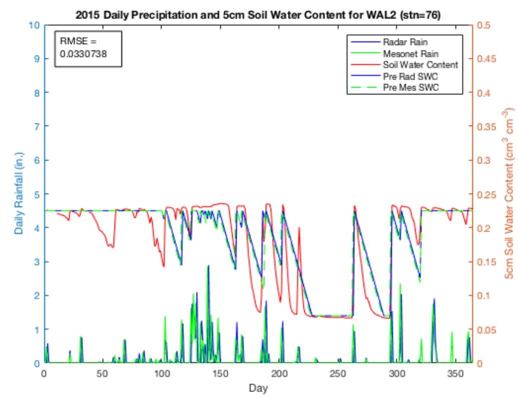
2015 Daily Precipitation and 5cm Soil Water Content for WAL2 (stn=76)
RMSE =
0.0330738
Radar Rain
Mesonet Rain
Soil Water Content
Pre Rad SWC
Pre Mes SWC
Daily Rainfall (in.)
5cm Soil Water Content (cm³ cm⁻³)
Day

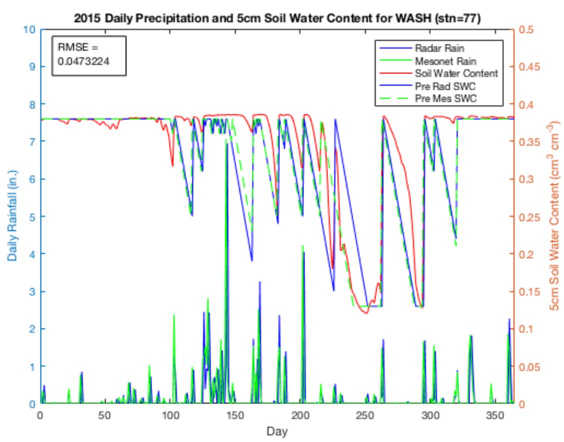
2015 Daily Precipitation and 5cm Soil Water Content for WASH (stn=77)
RMSE =
0.0473224
Radar Rain
Mesonet Rain
Soil Water Content
Pre Rad SWC
Pre Mes SWC
Daily Rainfall (in.)
5cm Soil Water Content (cm³ cm⁻³)
Day

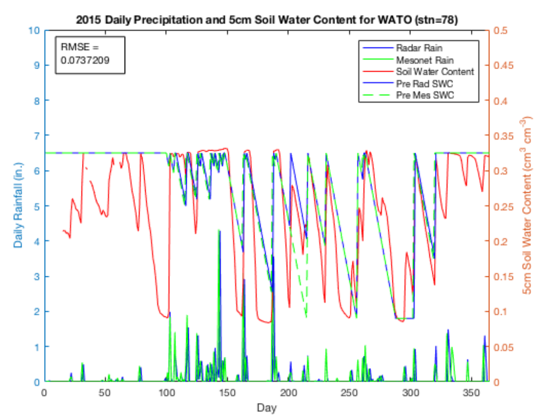
2015 Daily Precipitation and 5cm Soil Water Content for WATO (stn=78)
RMSE =
0.0737209
Radar Rain
Mesonet Rain
Soil Water Content
Pre Rad SWC
Pre Mes SWC
Daily Rainfall (in.)
5cm Soil Water Content (cm³ cm⁻³)
Day

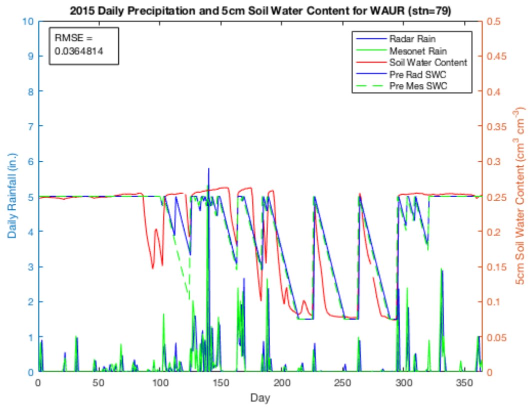
2015 Daily Precipitation and 5cm Soil Water Content for WAUR (stn=79)
RMSE =
0.0364814
Radar Rain
Mesonet Rain
Soil Water Content
Pre Rad SWC
Pre Mes SWC
Daily Rainfall (in.)
5cm Soil Water Content (cm^3 cm^-3)
Day

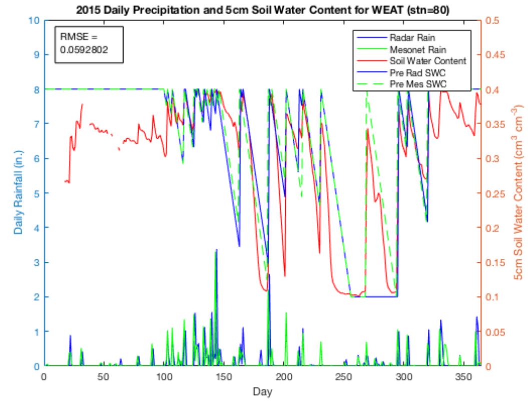
2015 Daily Precipitation and 5cm Soil Water Content for WEAT (stn=80)
RMSE =
0.0592802
Radar Rain
Mesonet Rain
Soil Water Content
Pre Rad SWC
Pre Mes SWC
Daily Rainfall (in.)
5cm Soil Water Content (cm^3 cm^-3)
Day

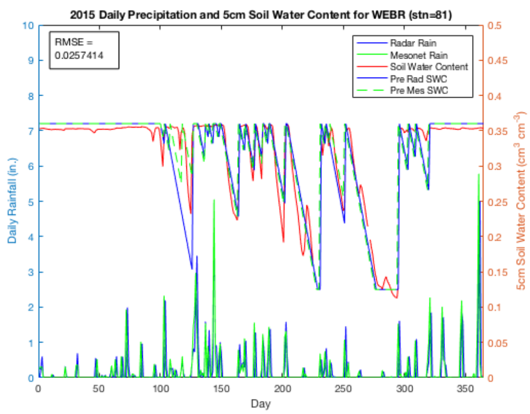
2015 Daily Precipitation and 5cm Soil Water Content for WEBR (stn=81)
RMSE =
0.0257414
Radar Rain
Mesonet Rain
Soil Water Content
Pre Rad SWC
Pre Mes SWC
Daily Rainfall (in.)
5cm Soil Water Content (cm^3 cm^-3)
Day

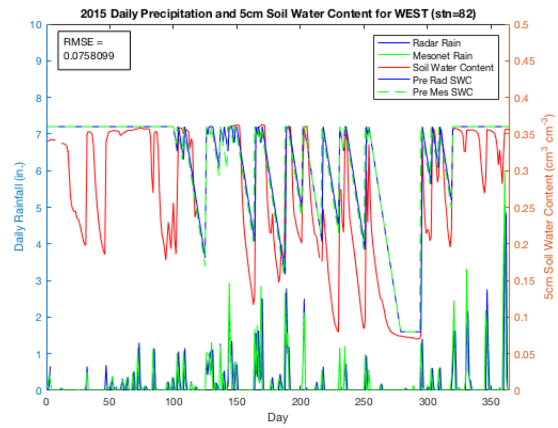
2015 Daily Precipitation and 5cm Soil Water Content for WEST (stn=82)
RMSE =
0.0758099
Radar Rain
Mesonet Rain
Soil Water Content
Pre Rad SWC
Pre Mes SWC
Daily Rainfall (in.)
5cm Soil Water Content (cm^3 cm^-3)
Day

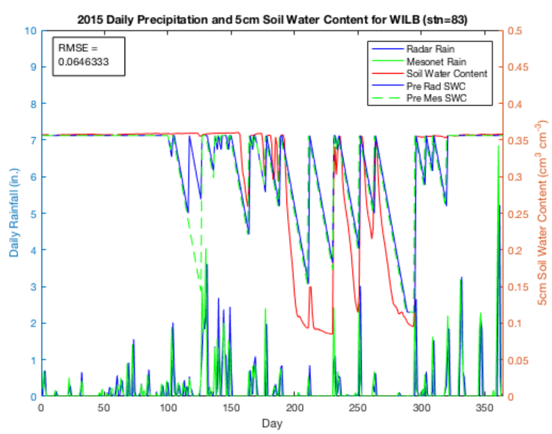
2015 Daily Precipitation and 5cm Soil Water Content for WILB (stn=83)
RMSE =
0.0646333
Radar Rain
Mesonet Rain
Soil Water Content
Pre Rad SWC
Pre Mes SWC
Daily Rainfall (in.)
5cm Soil Water Content (cm^3 cm^-3)
Day

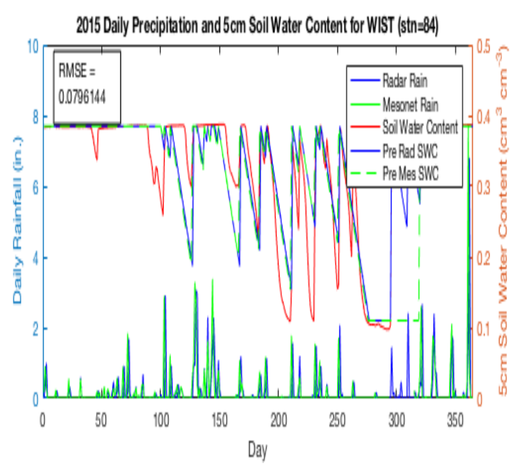
2015 Daily Precipitation and 5cm Soil Water Content for WIST (stn=84)
RMSE =
0.0796144
Radar Rain
Mesonet Rain
Soil Water Content
Pre Rad SWC
Pre Mes SWC
Daily Rainfall (in.)
5cm Soil Water Content (cm^3 cm^-3)
Day

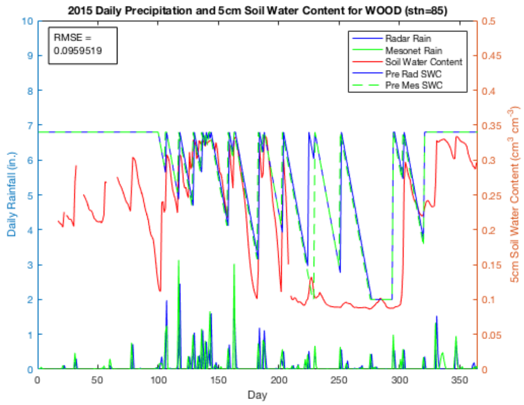
2015 Daily Precipitation and 5cm Soil Water Content for WOOD (stn=85)
RMSE =
0.0959519
Radar Rain
Mesonet Rain
Soil Water Content
Pre Rad SWC
Pre Mes SWC
Daily Rainfall (in.)
5cm Soil Water Content (cm³ cm⁻³)
Day

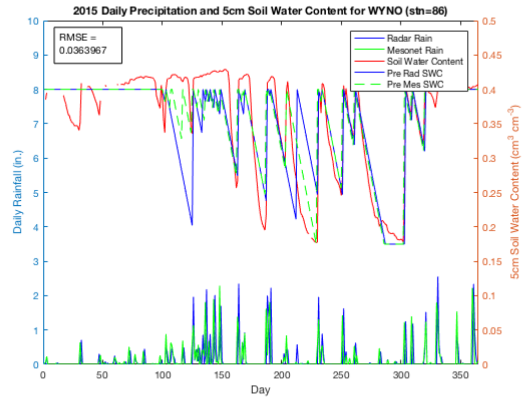
2015 Daily Precipitation and 5cm Soil Water Content for WYNO (stn=86)
RMSE =
0.0363967
Radar Rain
Mesonet Rain
Soil Water Content
Pre Rad SWC
Pre Mes SWC
Daily Rainfall (in.)
5cm Soil Water Content (cm³ cm⁻³)
Day

Appendix B

Soil water content for every day of 2015 at six locations in Florida. Red line is the soil moisture. Blue line is rainfall amount each day in inches times 2 and the green line the predicted soil moisture.